

**APPENDIX A**  
**Geochemical Assessment**

## **APPENDIX A**

### **Cameco Geochemical Modeling Report**



***Prepared for:***

Cameco Resources (USA)  
2020 Carey Avenue, Suite 600  
Cheyenne, Wyoming, 82001

***Prepared by:***



INTERA Incorporated  
6000 Uptown Boulevard NE, Suite 220  
Albuquerque, New Mexico 87110

**May 13, 2013**





## TABLE OF CONTENTS

<b>LIST OF FIGURES .....</b>	<b>ii</b>
<b>LIST OF TABLES .....</b>	<b>ii</b>
<b>LIST OF ATTACHMENTS .....</b>	<b>ii</b>
<b>ACRONYMS AND ABBREVIATIONS.....</b>	<b>iii</b>
<b>1.0 INTRODUCTION.....</b>	<b>1</b>
1.1 Conceptual Model .....	1
1.2 Regional Geology .....	1
1.3 Site-Specific Geology .....	2
1.4 Mineralogy of the Highland Sandstone Unit .....	2
1.5 Groundwater Flow System .....	3
1.6 Alterations to MU-B Geochemistry during ISR .....	3
1.7 Alterations to Geochemistry during Restoration .....	4
1.8 Current Redox Conditions .....	4
1.9 Current Production Area Constituent Distribution .....	5
<b>2.0 GEOCHEMICAL MODEL .....</b>	<b>5</b>
2.1 Code Description (PHREEQC).....	5
2.2 Conceptual Model.....	6
2.2.1 Particle Track Paths.....	7
2.3 Parameter Selection .....	7
2.3.1 Hydrogeologic Parameters .....	7
2.3.2 Reactive Minerals.....	8
2.3.3 Ion Exchange.....	9
2.3.4 Sorption Surfaces .....	9
2.3.5 Co-Precipitation of Barite and RaSO <sub>4</sub> .....	10
2.4 Attenuation Mechanisms .....	11
2.4.1 Attenuation Properties of Uranium .....	11
2.4.2 Attenuation Properties of Arsenic .....	12
2.4.3 Attenuation Properties of Selenium .....	13
2.4.4 Attenuation Properties of Radium.....	13
<b>3.0 MODELING RESULTS.....</b>	<b>13</b>
3.1 General Water Quality Parameters .....	13
3.2 Uranium .....	14
3.3 Arsenic .....	14
3.4 Radium.....	14
3.5 Conclusions.....	15
<b>4.0 REFERENCES.....</b>	<b>16</b>



## LIST OF FIGURES

Figure 1	Location Map
Figure 2	Mineralization Front for 30-Sand from Hunter, 1999
Figure 3	Modified Cross Section from Hunter, 1999
Figure 4	Schematic Diagram of Roll-Front Deposit
Figure 5	Projected 30-Sand Steady-State Water Level Elevation
Figure 6	pH pE Plot
Figure 7	Natural Neighbor Interpolation of Arsenic Groundwater Concentrations
Figure 8	Natural Neighbor Interpolation of Selenium Groundwater Concentrations
Figure 9	Natural Neighbor Interpolation of Radium 226 Groundwater Concentrations
Figure 10	Natural Neighbor Interpolation of Uranium Groundwater Concentrations
Figure 11	Particle Tracks Paths Generated from Steady-State Future Condition MODFLOW Model (Aqui-Ver, 2011)

## LIST OF TABLES

Table 1	Groundwater Velocities Used for Geochemical Transport Simulations.....	7
Table 2	Aquifer Parameters Used for Geochemical Transport Simulations.....	8
Table 3	Mineralogical Data from A-Wellfield Core Study for M-7 bore hole.....	9
Table 4	2005 Arsenic Speciation Data.....	12

## LIST OF ATTACHMENTS

Attachment A	PHREEQC Input Files
Attachment B	PHREEQC Graphical Output Constituent Concentration over Time at POE Wells for all Simulations



## ACRONYMS AND ABBREVIATIONS

1D	one-dimensional
ACL	alternate concentration limit
arsenic III	arsenite
arsenic V	arsenate
Cameco	Power Resources Incorporated dba Cameco Resources
CEC	cation exchange capacity
COC	constituents of concern
EPA	United States Environmental Protection Agency
GWS	groundwater sweep
HFO	hydrous ferric oxide
Highland Project	In-Situ Uranium recovery project at Highlands
HSU	Highland sandstone unit
ISR	In-Situ Recovery
MCL	Maximum Concentration Limit
meq/100g	milliequivalent per 100 gram
meq/L	milliequivalent per liter
mg/L	milligram(s) per liter
MU-B	Mine Unit-B
mV	millivolt(s)
ORP	oxidation reduction potential
pCi/L	picocuries per liter
POC	Point of Compliance
POE	Point of Exposure
RO	reverse osmosis
Se(IV)	selenite
Se(VI)	selenate
TDS	total dissolved solids
U(IV)	uranous
U(VI)	uranyl



## 1.0 INTRODUCTION

Geochemical modeling was conducted for the Power Resources Incorporated, d.b.a. Cameco Resources (Cameco), In-Situ Uranium recovery (ISR) project at Highlands (Highland Project), located in T36N R72W, Converse County, Wyoming (Figure 1). The purpose of this modeling was to determine the fate and transport of constituents in the Mine Unit-B (MU-B) production zones (Point of Compliance [POC]) as groundwater migrates downgradient to the monitoring well ring (hereafter referred to as the Point of Exposure [POE] well ring). Geochemical modeling can be useful in determining processes that affect constituents as they move from one geochemical environment to another. Results from this geochemical model will be used to demonstrate the probable fate of constituents as groundwater travels through the ISR zone over time.

### 1.1 Conceptual Model

This section presents our conceptual understanding of the model area including geology, hydrogeology, conceptual water budget, and geochemical setting.

### 1.2 Regional Geology

The Highland Project is located in the Powder River Basin, a structural and topographic basin that covers approximately 12,000 miles in the northeastern part of Wyoming. The basin and its surrounding uplifts were created by Laramide thrusting during Paleocene and Eocene times. Subsequent to deformation, sediment from surrounding uplifts filled the Powder River Basin. Gradual subsidence of the basin provided accommodation space for the accumulation of several thousand feet of fluvial floodplain sediments that now make up the Fort Union Formation. The formation and subsequent burial of backswamps in the late Paleocene and early Eocene allowed for the dewatering of organic-rich silts and clays, most likely through channel sands. The transport of these organic-rich fluids facilitated the reduction of minerals in Fort Union channel sands, transforming them to a uniform gray color. The Fort Union Formation was overlain by the Wasatch Formation in the Eocene, which was overlain by the White River Formation in the Oligocene. It is assumed that meteoric water percolated through the White River Formation before regional uplift in the Pliocene caused much of the formation to be eroded. Eventually, the meteoric water from the White River Formation percolated into the Fort Union Formation. The oxidizing meteoric water altered the host-rock, resulting in the dissolution and subsequent concentration and precipitation of heavy metals, particularly uranium. The patterns of host-rock alteration remain today, recording the infiltration of paleo-groundwater and subsequent geochemical changes to the host-rock (Hunter, 1999). The degree of oxidation of the host-rock varies by formation and geographic location (Figure 2).

### **1.3 Site-Specific Geology**

Previous studies (Langen and Kidwell, 1974; Dahl and Hagmaier, 1976, as referenced in Hunter, 1999) identified a group of three distinctive fluvial channel sandstones that contain most of the uranium in the Highland Project area. These studies named the fluvial sandstone the Highland sandstone unit (HSU). The HSU is 120 to 150 feet thick and is stratigraphically located in the Upper Fort Union Formation (Figure 3). The HSU crops out east of the Highland Project area and dips gradually basinward and westward to a depth of around 1,000 feet near the project area. At the Highland Project area, the fluvial sand members of the HSU are identified as the 30-Sand, 40-Sand, and 50-Sand, although other sand units are present in the area ranging from 10-Sand to 100-Sand (Figure 3). The sands are generally separated by silty claystone floodplain deposits, but may be in hydraulic communication in local areas if floodplain deposits are not present (Hunter, 1999). This study will consider the geochemical interactions of groundwater and matrix material in the 30-Sand near the Highland Project area, as the 30-Sand was the main production zone for Highland Project MU-B.

### **1.4 Mineralogy of the Highland Sandstone Unit**

Due to their similarity, the sedimentological and mineralogical properties of the three members of the HSU (30-Sand, 40-Sand, and 50-Sand) can be accurately described as one unit. The HSU is composed of fine to medium, coarse-grained, poorly lithified, arkosic sandstone typically ranging from 20 to 50 feet in thickness. Clastic grains are loosely bound in a matrix of clay with sparse calcite cement. Multiple erosion surfaces within the fluvial sand units indicate that they formed via vertical and lateral accretion of several meanderbelt stream deposits. Silty and clayey floodplain deposits were re-worked and washed downstream, along with associated vegetation. Larger woody-type organic matter was stranded on river bars, while smaller bits of organic matter were typically associated with channel lag deposits. While thin coal layers were deposited between the fluvial sand units, they are not present everywhere. Absence of the coal layers with entrainment of organic debris in the fluvial sands has been attributed to erosion of coal layers by overlying meanderbelt streams. Some of the interbedded and dispersed organic material underwent diagenesis to produce pyrite and gaseous emissions. It is this combination of pyrite, organic matter, and gaseous emissions that reduced incoming meteoric water and caused uranium and other heavy metals to precipitate out of solution. As oxidizing water encountered the reduction front, redox-sensitive metals were released into solution until they traveled far enough downgradient to be reduced by the unaltered formation and precipitated out of solution, creating the characteristic roll-front deposits seen in the Highland area (Figure 4). High-grade uranium ore is often mixed with coalified fragments, finely disseminated pyrite, and color-zoned clay nodules (Hunter, 1999). The geographic distribution of channel sands, floodplain deposits, and alteration zones for the 30-Sand can be seen in (Figure 2).



## **1.5 Groundwater Flow System**

Uranium has been recovered from the Highland Project area for 40 years using various recovery methods. Underground and open-pit recovery methods have significantly altered the pattern of groundwater flow in the Highland Project area. The general pattern of groundwater flow in the 30-Sand is toward the south and southeast across the MU-B area, with the large majority of MU-B groundwater flow ultimately captured by the Highland pit lake (Figure 5). However, projections show that a groundwater divide will exist along the northern boundary of MU-B in the 30-Sand aquifer, with the flow north of the divide ultimately discharging into the Box Creek drainage, and the flow south of the divide discharging into the Highland pit lake (Figure 5). The Highland pit lake is located southwest and downgradient of the MU-B production zone, and is currently a groundwater sink due to dewatering during operation. The Exxon underground facility is located to the northwest of the MU-B wellfield, and the Exxon open pit is projected to continue to be a sink due to evaporation losses in the pit lake. Currently, water flows away from MU-B in the direction of the piezometric low near the underground workings, but is expected to reverse and flow towards MU-B over time as the potentiometric surface near the underground mine recovers. Consequently, there is potential for water from the underground workings to migrate into the wellfield over time (Aqui-Ver, 2011).

## **1.6 Alterations to MU-B Geochemistry during ISR**

The roll-front deposits at MU-B were recovered from the 30-Sand using ISR techniques, therefore, the 30-Sand may be affected by transport of constituents of concern (COCs) due to ISR of uranium. Because the 20-Sand is hydraulically connected to the 30-Sand in the northwestern portion of MU-B (Appendix B of the ACL Report, INTERA, 2013), it is possible that some small amounts of COCs may be transported within the 20-Sand due to activity in the 30-Sand. However, previous work by Lewis (2001) has shown that significant attenuation will take place in the 20-Sand as groundwater moves toward the POE. ISR consists of installing several patterns of groundwater wells. Generally, each pattern is a “five spot pattern,” consisting of one production well surrounded by four injection wells (Figure 2). During the ISR process, groundwater is pumped from the formation, and oxygen, carbon dioxide, or sodium bicarbonate is added to the native groundwater. The injected water travels through the aquifer from the potentiometric high at the injection well to the potentiometric low at the central production well. As the oxidizing solution moves through the aquifer, it acts on the reduced minerals in the roll-front deposits, releasing uranium and other constituents into solution. The soluble uranium is complexed by the carbonate that was added to the water, keeping the uranium in solution during the ISR process. The water is then pumped to the surface, and the uranium is removed from the solution using ion-exchange resin, which adsorbs the uranium from the solution. Once the uranium is removed from the groundwater, the water is fortified with oxygen, carbon dioxide,



and/or sodium bicarbonate and returned to the wellfield where it is reinjected into the formation except for the removal of a bleed stream (typically 1% of the total flow) to provide hydraulic control of the mining solutions. This process repeats until the mine unit ceases production.

### **1.7 Alterations to Geochemistry during Restoration**

After ISR operation ceased, the groundwater restoration for MU-B began. The first step in the restoration process was to sample the MP Wells using the approved constituent list from the NRC License SUA-1548 and WDEQ permit No. 603 to establish post-ISR groundwater quality. Following post-ISR groundwater sampling, restoration began with groundwater sweep (GWS), which consisted of pumping the production wells without injection. GWS is designed to pull the water that has been affected by ISR into the center ISR patterns, which began reducing the TDS in the mine unit. Typically the GWS consists of at least one pore volume. The next phase of the restoration process, called reverse osmosis (RO) sweep, consisted of pumping the water from the mine unit, treating the groundwater with an RO filter, and reinjecting the clean water back into the wellfield to further reduce the TDS and other constituents in the affected formation. The final restoration step was reductant addition, which is designed to introduce reducing conditions to the formation and stop the ISR process. MU-B had two methods of reductant addition employed during the restoration process. Part of the mine unit received sodium sulfide, a powerful chemical reductant, and the whole mine unit received biological amendments. In general, the restoration efforts served to re-establish reducing conditions in the MU-B production zone. A reduced environment can help redox-sensitive metals such as uranium to precipitate from solution if sufficient concentrations of other dissolved solids are present to form a solid-phase mineral. In addition, RO treatment helped to remove much of the dissolved solids, particularly anions like sulfate and chloride, from solution. A more detailed summary of restoration efforts is provided in Cameco (2009).

### **1.8 Current Redox Conditions**

Oxidation reduction potential (ORP) conditions were measured at several monitoring and injection wells during the last quarter of 2011 during sampling using two different sampling techniques. ORP was measured with an in-situ sonde for injection wells, while downhole groundwater pumps outfitted with flowthrough cells were used for monitoring (POE and POC) wells. ORP measurements were converted to pE and then plotted against pH in order to adequately understand redox conditions. Although determination of redox conditions using a well-established redox couple would be preferable, that data does not exist, and therefore field ORP measurements are the best available data. Plotting of the data showed two distinct groupings of redox conditions (Figure 6). The differences in redox conditions could be attributed to actual differences in condition or differences in measurement methods that were employed on

each well type. It is notable that the lowest redox potentials occur in injection wells, suggesting that injected reducing agents may have preferentially reduced areas around injection wells.

### **1.9 Current Production Area Constituent Distribution**

Analytical data from field sampling in the fourth quarter of 2011 was joined with spatial data in ArcGIS and plotted on a basemap. Because the 2011 data did not completely cover the MU-B ISR area, values from baseline sampling were added in the perimeter ring to provide adequate control points for interpolation of values. Baseline data were not used where POE well data from 2011 were present. The values for each COC were interpolated using the Natural Neighbor method (Figures 7-10). The Natural Neighbor method generates a localized interpolation, using only sample points that surround a query point, guaranteeing that the interpolated values will always be within the range of the interpolated points. In general, concentrations were higher in the POC wells (MP-Wells) and lower in the POE wells (M-Wells). Only field conditions were measured at injection wells (I-Wells), although redox data would seem to suggest that heavy metals concentrations may be lower in the injection wells. Most constituents were concentrated in two general areas. A group of wells on the northern side of the wellfield consisting of MP-31, MP-30, MP-19, MP-16, MP-14, and MP-12 generally contained higher concentrations of constituents, while MP-26 and MP-27 had higher concentrations on the southern side of the wellfield. Detailed distributions of alternate concentration limit (ACL) constituents are easily interpreted in spatial format (Figures 7-10).

## **2.0 GEOCHEMICAL MODEL**

### **2.1 Code Description (PHREEQC)**

PHREEQC version 2 is a computer program written in the C programming language that is designed to perform a wide variety of low-temperature, aqueous, geochemical calculations. PHREEQC is based on an ion-association aqueous model and has capabilities for:

1. Speciation and saturation-index calculations.
2. Batch-reaction and one-dimensional (1D) transport calculations involving:
  - a. Reversible reactions, including aqueous, mineral, gas, solid-solution, surface-complexation, and ion-exchange equilibria.
  - b. Irreversible reactions, including specified mole transfers of reactants, kinetically controlled reactions, mixing of solutions, and temperature changes.

3. Inverse modeling, which finds sets of mineral and gas mole transfers that account for differences in composition between waters, within specified compositional uncertainty limits.

New features in PHREEQC version 2 relative to version 1 include capabilities to:

- Simulate dispersion (or diffusion) and stagnant zones in 1D-transport calculations.
- Model kinetic reactions with user-defined rate expressions.
- Model the formation or dissolution of ideal, multicomponent or nonideal, binary solid solutions.
- Model fixed-volume gas phases in addition to fixed-pressure gas phases.
- Allow the number of surface or exchange sites to vary with the dissolution or precipitation of minerals or kinetic reactants.
- Include isotope mole balances in inverse modeling calculations.
- Automatically use multiple sets of convergence parameters.
- Print user-defined quantities to the primary output file and (or) to a file suitable for importation into a spreadsheet.
- Define solution compositions in a format more compatible with spreadsheet programs.

## 2.2 Conceptual Model

The model simulates low total dissolved solids (TDS) water from upgradient of MU-B flushing through the ISR zone of the 30-Sand, which has a higher amount of dissolved solids. Chemistry data from an upgradient POE well is used for the incoming solution, while a mineralized zone POC well is used for the ISR zone solution. Each 50-meter cell in the transport model is adjusted to contain the minerals most like those that would be present at its location along the track path (Figure 2). The facies shown on Figure 2 in map view correspond in a general sense to the mineral assemblages shown in cross-section in Figure 4, with the roll-front (the interface of reduced and oxidized zones) being located near the downgradient (east) edge of the alteration zone in Figure 2. Mineralogical studies from Mine Unit K (Cameco, 2007) were also used as a guide for developing mineral assemblages. A POE well is used to simulate the reduced portions of the aquifer to simulate conditions downgradient of the mineralized (production) zone. Simulations are projected to the POE, although a particle of water may travel a significant distance past the POE before being discharged from the groundwater system (Figure 11).

### 2.2.1 Particle Track Paths

Several particle track paths were generated using the steady-state future prediction for the 30-Sand aquifer from the (Aqui-Ver, 2011) model. The track paths simulate the path of a particle of water as it moves from upgradient, through the ISR zone (POC wells), past the outer POE well, and ultimately to its discharge location. Geochemical modeling is conducted only from the upgradient POE well to the downgradient POE well. Results indicate that the average groundwater velocity ranges from 5.2 to 10.7 feet/year for the eight contaminant sources along their pathlines (Table 1). Of the chosen particles, four will discharge at the Highland pit lake, while one will eventually discharge at Box Creek. Track paths were chosen that would intersect with an area of high concentration so that results would represent a worst case scenario (Figures 7-10). Data from the track paths is used to create a geochemical transport model in PHREEQC.

**Table 1**  
**Groundwater Velocities Used for Geochemical Transport Simulations**

Upgradient POE Well	POC Well	Downgradient POE Well	Maximum Groundwater Velocity (feet/year)	Minimum Groundwater Velocity (feet/year)	Average Groundwater Velocity (feet/year)
M-56	MP-12	M-24	50.69	1.84	8.52
M-55	MP-16	M-24	12.38	1.57	5.21
M-63	MP-21	M-36	19.06	3.82	7.96
M-45	MP-27	M-38	19.13	5.19	10.66
M-44	MP-26	M-37	17.44	5.28	9.88

## 2.3 Parameter Selection

### 2.3.1 Hydrogeologic Parameters

The model uses the TRANSPORT module of PHREEQC code to simulate the effects of physical processes such as advection, dispersion, and diffusion in concert with chemical processes such as dissolution, precipitation, ion-exchange equilibria, solution mixing, and surface complexation reactions. Input parameters chosen for this module include boundary conditions, groundwater velocities, and longitudinal dispersivities (Table 2). To match the conceptual model, boundary conditions were chosen to be constant on the upgradient side of the simulation, and flux (conservation of mass) on the downgradient end of the simulation. The assumption of constant quality upgradient water may have to be reconsidered if water quality is significantly altered by the Exxon underground facility located upgradient of MU-B. Longitudinal dispersivities are calculated for each track path using the formula from Xu and Eckstein (1995). Groundwater



velocities, obtained from the results of the MODFLOW model, are modified for use in the PHREEQC model by calculating how long it takes a particle of water to cross a model cell of given length (timestep).

**Table 2**  
**Aquifer Parameters Used for Geochemical Transport Simulations**

Upgradient POE Well	POC Well	Downgradient POE Well	Track Path Length (meters)	Longitudinal Dispersivity (meters)	Timestep (s) for 50-m Cells	Number of Cells
M-56	MP-12	M-24	604	9.8	607433787	12
M-55	MP-16	M-24	759	10.7	993346615	15
M-63	MP-21	M-36	1101	12.2	650167822	22
M-45	MP-27	M-38	500	9.12	485491169	10
M-44	MP-26	M-37	468	8.89	523819419	9

### 2.3.2 Reactive Minerals

In order to simulate the subsurface mineralogy along the particle track paths present at MU-B, the track paths were overlayed with a facies map in ArcGIS (Hunter, 1999). Each 50-meter cell in the transport model is adjusted to contain the minerals most like those that would be present at its location along the track path (Figure 2). The facies shown on Figure 2 in map view correspond in a general sense to the mineral assemblages shown in cross-section in Figure 4, with the roll-front (the interface of reduced and oxidized zones) being located near the downgradient (east) edge of the alteration zone in Figure 2. Mineralogical studies from Mine Unit K (Appendix E of the ACL Application, INTERA, 2013) were also used as a guide for developing mineral assemblages. Three general sets of mineral assemblages were used to simulate mineralogical conditions: oxidized areas, transition areas, and reduced areas. Oxidized and reduced areas are used to represent those areas that are upgradient and downgradient of the oxidation front, respectively. Some reduced areas are actually upgradient of the oxidation front due to the alteration of the flow path between the time of initial oxidation and post ISR (Figure 2). Transition areas are intended to represent conditions closely upgradient of the oxidation front. All three mineral assemblages include quartz, k-feldspar, and k-montmorillonite. The transition zone assemblage also includes uraninite, coffinite, siderite, and goethite. Goethite is an important sorption surface for many of the constituents considered at the site, as described in Section 2.3.4 Sorption Surfaces. The reduced zone mineralogy contains quartz, k-feldspar, and pyrite, while the following mineral phases are allowed to precipitate if they become oversaturated: uraninite, coffinite, calcite, ferroselite, siderite, gypsum, and native selenium. In addition, radium and barium sulfate were placed in the mineral assemblage in the reduced zone cells to allow for (Ra,Ba)SO<sub>4</sub> co-precipitation when oversaturated. A more detailed explanation

of co-precipitation follows below. The amount of these minerals present initially is consistent with the abundance in the aquifer matrix, the amount of mineral surface available for reaction, and their solubility in water. Pyrite was included in the reactive minerals because it occurs throughout the mineralized area and plays a vital role in redox processes. The amounts of minerals present in each cell, along with all other model inputs, can be viewed in the PHREEQC input files (Attachment A).

### 2.3.3 Ion Exchange

Ion exchange surfaces are calculated based on mineralogical data that were collected from the A-Wellfield. Cation exchange capacity (CEC) was measured in milliequivalents per 100 grams (meq/100g) aquifer matrix for a core that was collected from the M-7 well in the A-Wellfield, and then converted to a milliequivalent per liter (meq/L) solution. The mineralogical data from the A-Wellfield is included in Table 3, below. A water-filled porosity of 21.8% and bulk density of 2.07 grams per cubic centimeter were used for this conversion. Bulk density was calculated based on an all quartz matrix, while porosity was obtained from a study conducted on another nearby Cameco ISR facility, Mine Unit K (Cameco, 2007). Cation exchange values were converted from meq/100g soil to meq/L of porewater solution for input to PHREEQC, following the methodology outlined in the frequently asked questions section of the PHREEQC webpage (Parkhurst, FAQs, 1999) to arrive at a value of .7 meq/liter of solution. Due to the lack of available data, and in order to provide conservative modeling results, the exchange constant for barium was used for the radium ion exchange processes.

**Table 3**  
**Mineralogical Data from A-Wellfield Core Study for M-7 Bore Hole**

Sample ID	CEC	Total Organic Carbon (meq/100g)	Pyrite % by volume	Clay % by volume
Composite	7.43	0.07	0.015	7
501-502	20	0.11		
505-506	5.87	0.14		
510-511	6.34	0.01		
513-514	4.33	0.02		
515-516	10.1	0.05		

### 2.3.4 Sorption Surfaces

The sorption mechanism involves protonation/deprotonation and complexation reactions on surface sites. Goethite was assumed to have properties similar to those of hydrous ferric oxide (HFO), and is considered to be more realistic than HFO for natural systems. Sorption of radium

and arsenic, along with the major cations and anions included in the `lnl.dat` database, were modeled to provide a realistic representation of the competition for surface sites on goethite. Research has shown that carbonate anions can significantly influence the sorption of arsenic onto HFO (Appelo, 2002). Accordingly, surface complexation of the carbonate anion on HFO was modeled as well. Surface-complexation constants for arsenate sorption on “weak” sites were obtained from Dzombak and Morel (1990), while the constants for radium and calcium were taken from Bassot et al. (2001). The equilibrium constants for arsenic fluoride species that were included in the `lnl.dat` database were unrealistic and caused unrealistically low amounts of arsenic sorption on HFO. To address this problem, the equilibrium constants for arsenic fluoride species were adjusted until they composed an insignificant fraction of arsenic species. Modeling studies by Smedley et al. (2002, p. 269) suggested that these species are minor, even with high arsenic and fluoride concentrations. The surface area of goethite per liter of porewater was related to the mass of goethite using a specific surface area of  $600 \text{ m}^2 \text{ g}^{-1}$  ( $5.33\text{e}4 \text{ m}^2 \text{ mol}^{-1}$ ). The concentrations of weak and strong sites were assumed to be 0.2 and 0.005 mol per mol of goethite, respectively. The mass of goethite, like that of any other mineral phase in the model, is subject to change by dissolution and precipitation with changing conditions.

### 2.3.5 Co-Precipitation of Barite and $\text{RaSO}_4$

Most source term calculations for Ra (II) pessimistically assume that its solubility is controlled by the individual solubility of  $\text{RaSO}_4(\text{s})$ , the most insoluble phase under near field conditions, while abundant information from early radiochemical research, natural system studies, and anthropogenic systems would indicate that Ra (II) behavior is largely determined by  $\text{BaSO}_4(\text{s})$  precipitation (SKB, 2008). Modeling the removal of Ra (II) from solution by precipitation of  $(\text{Ra,Ba})\text{SO}_4$  will allow for removal of far more Ra (II) than by precipitation of pure  $\text{RaSO}_4$ . However, as with any equilibrium-based solubility calculations, the stability of the co-precipitated compound will be dependent on the stability of the main components of the compound (Ba and  $\text{SO}_4$  in this case). Should the aqueous concentrations of either constituent diminish such that the co-precipitate is undersaturated, it is possible that Ra (II) can dissolve as the co-precipitated solid attempts to maintain equilibrium with the solution. For samples that tested below the detection limit of .1 milligram per liter (mg/L) for barium, a value of .02 mg/L was substituted. This value was obtained by allowing a small amount of barite to come to equilibrium with the solution under field measured conditions and using that as the initial input for the system. The two most prominent ways for dissolution of the co-precipitated solid to occur are: (1) acidification ( $\text{pH} < 3$ ) or alkalization ( $\text{pH} > 12$ ), and (2) bacterially promoted sulphate reduction. While acidification and alkalization present little risk at MU-B (Attachment A), sulfate-reducing bacteria were used as part of the restoration process, and could begin to flourish if conditions were favorable for their growth in the aquifer.

In order to model the removal of Ra (II) from solution by co-precipitation with barite, the Solid Solutions module in the geochemical code PHREEQC (Parkhurst and Appelo, 1999) was used. The Solid Solutions module allows for the co-precipitation of two solid phase minerals using thermodynamic data as defined in the database file (lntl.dat). The user can define several different methods to characterize the ideal vs. non-ideal behavior of the solid solution. Because Ra (II) has very similar size and charge to Ba (II), the crystal size and structure of pure  $\text{RaSO}_4$  is nearly identical to that of pure  $\text{BaSO}_4$ . It follows that the distribution of the tracer (Ra (II)) in the solid solution follows very nearly to Raoultian (Ideal) behavior, with the standard states defined as unit activity for the end member components (Zhu, 2004). Ideal behavior of the  $(\text{Ra,Ba})\text{SO}_4$  solid solution is assumed in this model.

## 2.4 Attenuation Mechanisms

### 2.4.1 Attenuation Properties of Uranium

Uranium occurs in +4, +5, and +6 oxidation states. Most important in nature are the uranous [U(IV)] and uranyl [U(VI)] oxidation states. U(IV), more common in waters with a low Eh and pH, tends to be strongly partitioned to solid phase U(IV) minerals such as uraninite and coffinite under most natural conditions. U(VI), found in more oxidizing waters with a pH greater than 5, tends to be much more mobile than U(IV) due largely to the high solubility and stability of uranyl (U(VI)) carbonate complexes. The most important U(VI) complexes are carbonate complexes, although U(VI) complexes with fluoride, phosphate, and sulfate can also affect uranium transport behavior (Langmuir, 1997).

Adsorption-desorption reactions are an important consideration for uranium behavior in natural environments. For most environmental conditions, dissolved uranium and other trace elements will always partition themselves between the water and the surfaces of contacting solids in soils, sediments, and rocks. In most groundwater systems ( $\text{pH} > 5$ ) more than 99% of individual trace elements will be associated with solid surfaces and less than 1% will be associated with dissolved surfaces. Because of their common occurrence in soils and sediments and strong sorptive behavior toward U(VI), the Fe(III) oxyhydroxides are generally the most important potential sorbents for uranium, with organic matter (peat, for example) second in importance (Langmuir, 1997). Once U(VI) has been adsorbed, it can be reduced to U(IV) in uraninite or coffinite by mobile reductants (such as  $\text{Fe}^{2+}$ ), or the adsorbent itself if it is organic matter. If reduction does not follow adsorption, the uranium can be desorbed by an increase of alkalinity at constant pH or by raising the pH. Such changes increase the extent of uranyl carbonate complexing, which is poorly adsorbed, causing desorption and remobilization of uranyl species.

Recent studies show that the presence of dissolved calcium can significantly alter the transport properties of uranium by inducing the formation of ternary uranyl-calcium-carbonate complexes

(Stewart, 2008). The speciation of dissolved U(VI) is skewed significantly towards these ternary complexes under most environmental conditions in the presence of dissolved calcium. Results indicate that there will be some reduction in the attenuation of dissolved complexed U(VI). However, experimental data for these species are not as available as those for uranyl carbonate complexes. The behavior of uranyl-calcium-carbonato complexes is not included in this model. The current uranium distribution in the 30-Sand is shown in Figure 10.

#### 2.4.2 Attenuation Properties of Arsenic

Arsenic is a redox-sensitive element. As a result, arsenic may be present in a variety of redox states. Arsenate (arsenic-V) and arsenite (arsenic-III) are the two forms of arsenic commonly found in groundwater (Masscheleyn et al., 1991). Arsenate generally predominates under oxidizing conditions. Arsenite predominates when conditions become sufficiently reducing. Under the pH conditions of most groundwater, arsenate is present as the negatively charged oxyanions  $\text{H}_2\text{AsO}_4^-$  or  $\text{HAsO}_4^{2-}$ , whereas arsenite is present as the uncharged species  $\text{H}_3\text{AsO}_3^0$  (Hem, 1985). Groundwater samples from Wells MP-14, MP-21, and MP-22 (production area wells with the highest arsenic concentrations) were analyzed at an offsite laboratory (Energy Laboratories, Inc.), and the arsenic in solution was determined to be primarily in the +3 valence state (Table 4).

**Table 4**  
**2005 Arsenic Speciation Data**

Sample Date	Well ID	Arsenic-III (mg/L)	Arsenic-V (mg/L)
03/23/2005	MP-14	0.13	0.0068
03/23/2005	MP-21	0.4	0.01
03/23/2005	MP-22	0.27	0.014

Arsenate and arsenite adsorb to surfaces of a variety of aquifer materials, including iron oxides, aluminum oxides, and clay minerals. Adsorption and desorption reactions between arsenate and iron-oxide surfaces are particularly important controlling reactions because iron oxides are widespread in the hydrogeologic environment as coatings on other solids, and because arsenate adsorbs strongly to iron-oxide surfaces in acidic and near-neutral-pH water (Dzombak and Morel, 1990; Waychunas et al., 1993). Iron-oxide surfaces also adsorb arsenite, and both arsenate and arsenite adsorb to aluminum oxides and clay-mineral surfaces. However, these adsorption reactions appear generally to be weaker than is the case for arsenate adsorption to iron-oxide surfaces under typical environmental pH conditions (Manning and Goldberg, 1997). Nevertheless, pH-dependent adsorption and desorption reactions other than those between arsenate and iron-oxide surfaces may be important controls over arsenic mobility in some settings.



### 2.4.3 Attenuation Properties of Selenium

Like arsenic, selenium is a redox sensitive element. As a solid phase, selenium is commonly present as Se (native selenium),  $\text{FeSe}_2$ , and  $\text{FeSe}$ , commonly in association with sulfur-containing minerals. In natural aqueous environments, selenium may be present in -2, +4, and +6 valence states. Selenium occurs in natural waters most commonly as selenite  $\text{Se(IV)}$  and selenate  $\text{Se(VI)}$ . Under reducing conditions, selenium tends to be immobile. Selenium tends to be strongly partitioned to sulfide minerals, metal oxide minerals, and organic matter. Maximum adsorption of selenate and selenite occurs primarily through specific adsorption in the acidic pH range on geologic materials enriched in hydrous oxides of Al and Fe or amorphous aluminosilicates. Sulfate is reported to compete for Se adsorption sites.  $\text{Se(VI)}$  is only weakly adsorbed by oxides and clays at near-neutral pH. Hence, oxidation of  $\text{Se(IV)}$  to  $\text{Se(VI)}$  enhances selenium mobility and persistence in natural waters.

### 2.4.4 Attenuation Properties of Radium

Radium-226 and radium-228 are products of the uranium-238 and thorium-232 decay chains, respectively. However, once in solution, these isotopes display the same geochemical behavior as all other radium ions. Radium, present in solution almost exclusively as  $\text{Ra}^{2+}$  ion, is soluble only under acid conditions and is generally immobile in natural waters due to the extreme insolubility of radium sulfate (Brookins, 1988). Radium-226 typically comprises more than 90% of total radium. Figure 9 shows the Radium-226 distribution in the 30-Sand, with Radium-226 present above 5 picocuries per liter (pCi/L) in some areas. However, radium-226 was present above 5 pCi/L in many of these areas during the baseline monitoring period, especially nearer to the ore body. Additionally, radium is commonly attenuated via co-precipitation with barium and sulfate (barite) (SKB, 2008).

## 3.0 MODELING RESULTS

Transport model simulations were conducted using aqueous analytical data from the fourth quarter of 2011 (Attachment B) and aquifer matrix parameters from the nearby A-Wellfield (Table 3). Tables 1 and 2 show the hydrogeologic parameters used for each track path. Model results are discussed in a general fashion in the text, with results for individual track paths shown in Attachment A.

### 3.1 General Water Quality Parameters

Careful monitoring of modeled general water quality parameters is one way to monitor the integrity of the geochemical model. Field measured pH values for M and MP-Wells ranged from 6.7-8.0, while modeled pH values ranged from 7.0 to 7.2 (Attachment A) for the conditions in

the 30-Sand aquifer. Field measured pE conditions ranged from 0 to 3 millivolts (mV) for all M and MP-Wells (Figure 6), while modeled pE values were near to -3.5 mV for all simulations. The difference between modeled and measured pE values is due to the solution reacting to redox equilibrium with the pure solid phase minerals in each cell. However, the modeled pE values may actually be more representative of redox conditions due to the difficulty associated with collecting representative pE measurements in the field.

### 3.2 Uranium

Uranium concentrations are predicted to remain very constant at the POE wells, with concentrations remaining near  $1 \times 10^{-4}$  mg/L throughout the entire simulation period for all simulations. In all cases, aqueous uranium concentrations are controlled by precipitation and dissolution of uraninite in the reduced zone cells. Modeled uranium concentrations were higher near the POC wells during simulations due to higher ambient uranium concentrations and the presence of solid phase uraninite in those model cells that represent the partially recovered uranium mineralization. Uraninite was not initially present in the downgradient cells, but was allowed to precipitate if it became oversaturated.

### 3.3 Arsenic

Although speciation data would suggest that arsenic could form relatively insoluble sulfide minerals, including orpiment and realgar, the concentrations of arsenic and sulfides were not high enough to play a significant role in arsenic attenuation. Results for arsenic in the model were, however, highly dependent on the amount of goethite that was specified to be present just upgradient of the reduced sections of the aquifer. Arsenic concentrations at the POE are below the United States Environmental Protection Agency (EPA) Maximum Concentration Limit (MCL) of 0.05 mg/L for all simulations when .01 moles of goethite is specified to be present in the aquifer matrix (Attachment A).

### 3.4 Radium

Radium concentrations at the POE wells are primarily affected by ion exchange along the flow path, with some additional effect provided by co-precipitation of  $\text{RaSO}_4$  with  $\text{BaSO}_4$ . When only modeled with advection and dispersion, high radium concentrations moved from the ISR area to downgradient in a tight "slug" pattern, dropping to near upgradient concentrations after the high concentration slug passes through the POE well. With the addition of ion exchange processes, the high concentration slug is avoided. However, the radium concentrations remain elevated, relative to upgradient levels, throughout the entire simulation. Because ion exchange is an equilibrium-based process, it is reversible if conditions change. Radium that is initially stored on exchangers due to contact with high concentrations of radium in ISR areas is released into



solution as lower concentration waters from upgradient interact with the exchange surface. The combination of ion exchange and co-precipitation of  $(\text{Ra}, \text{Ba})\text{SO}_4$  results in additional lowering of the amount of radium in solution, lowering dissolved concentrations at the POE (Attachment A).

### 3.5 Conclusions

Geochemical modeling indicates that there will be a reduction in constituent concentrations in groundwater over time and over distance from the POC (source) area. Based on current mineral distributions in the aquifer and future steady-state predictions of flow conditions, the concentrations of dissolved constituents at the modeled POE are predicted to remain below the site-specific, health-risk-based standards of 31 pCi/L for radium 226+228, and 0.09 mg/L for uranium, while concentrations will remain below the regulatory-based limits of 0.01 mg/L and 0.05 mg/L (Appendix A to 10 C.F.R. 40.5C, 2012) for selenium and arsenic, respectively. The concentrations are predicted to remain under these concentration limits for the duration of the 1,000-year modeling period.

## 4.0 REFERENCES

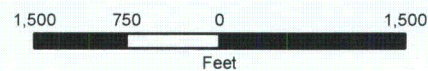
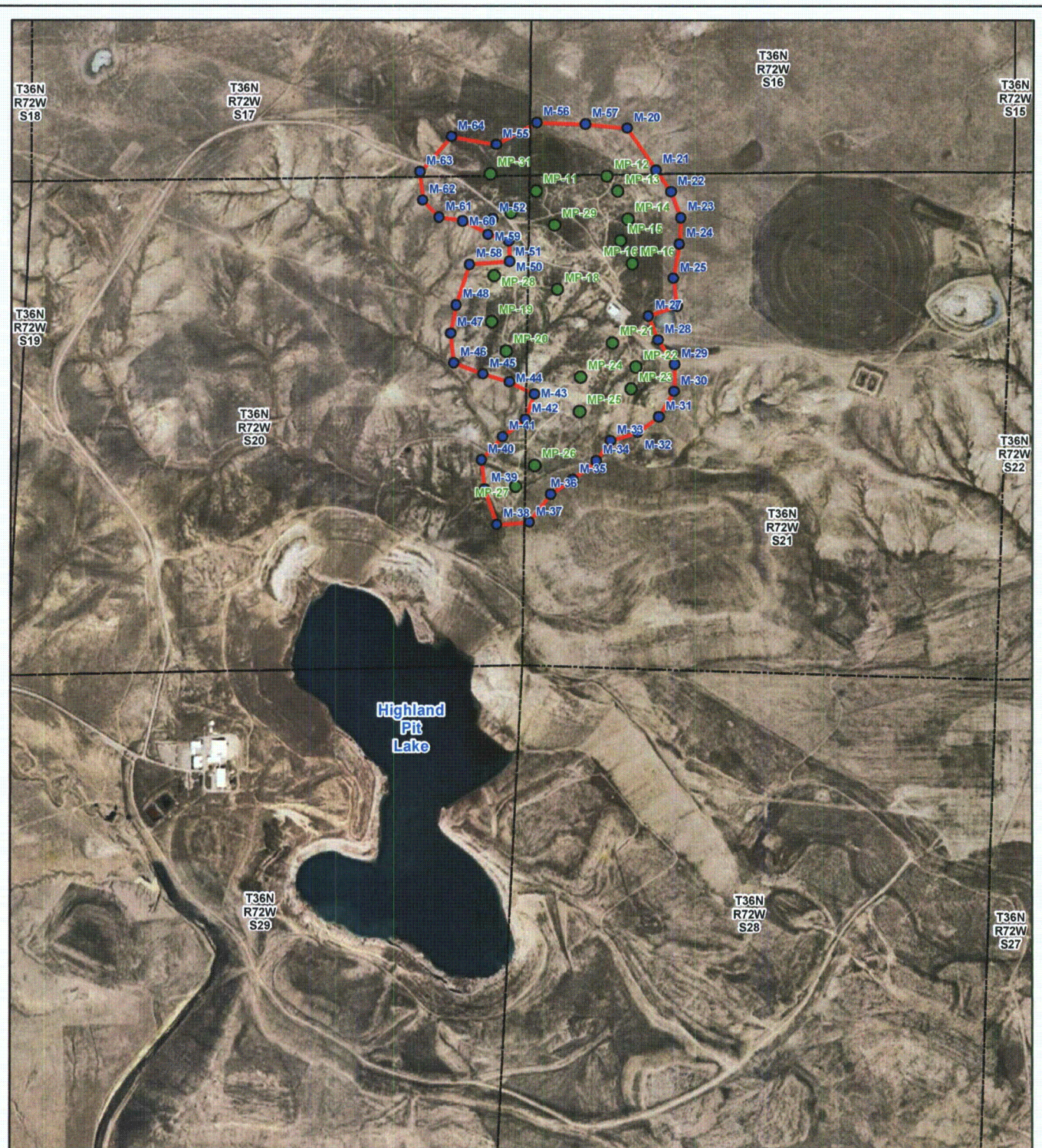
- Appelo, C.A.J., M.J.J. van der Weiden, C. Tournassat, and L. Charlet, 2002. "Surface Complexation of Ferrous Iron and Carbonate on Ferrihydrite and the Mobilization of Arsenic." *Environmental Science and Technology*, Volume 36, No. 14, p. 3096-3103.
- Aqui-Ver Inc., 2011. Mine Unit B Hydrologic Assessment, Cameco Resources Highland Uranium Project, Converse County, Wyoming.
- Bassot, S., C. Mallet, and D. Stammose, 2001. Experimental Study and Modeling of the Radium Sorption onto Goethite. *Materials Research Society Symposium Proceedings*, Volume 663.
- Brookins, D.G., 1988. *Eh-pH Diagrams for Geochemistry*. Springer-Verlag, New York, New York, 176 pp
- Cameco Resources, 2009. MU B Ground Water Submittal. Cameco Resources, Smith Ranch-Highland Operation. Includes: Restoration Report, Correspondence, Stability Report, Final Report – WDEQ.
- Cameco Resources, 2007. Mine Unit K Leach Study – Final Report. Report No. TD 07-05. June.
- Dahl, A.R. and Hagmaier, J.L., 1976. Genesis and Characteristics of the Southern Powder River Basin Uranium Deposits, Wyoming. *Wyoming Geological Association, 28th Annual Field Conference Guidebook*, p.243-252.
- Dzombak, D.A. and F.M.M. Morel, 1990. *Surface Complexation Modeling: Hydrous Ferric Oxide*. New York: John Wiley & Sons, 393 p.
- Hem, J.D., 1985. *Study and Interpretation of the Chemical Characteristics of Natural Water*, 3rd ed., U.S. Geological Survey Water-Supply Paper 2254, 263 p.
- Hunter, John, 1999. Fluvial Architecture and Paleo-Ground Water Infiltration of the Fort Union Formation near the Highland Uranium Mine, Southern Powder River Basin, Wyoming. *Wyoming Geological Association. Coalbed Methane and Tertiary Geology of the Powder River Basin, Wyoming and Montana, 50<sup>th</sup> Annual Field Conference Guidebook*, 1999.
- INTERA, 2013. Application for Alternate Concentration Limits for the Smith Ranch-Highland Mine Unit-B In-Situ Uranium Recovery Facility, Converse County, Wyoming. Prepared for Cameco Resources (USA). May.
- Langen, R.E. and A.L. Kidwell, 1974. "Geology and Geochemistry of the Highland Uranium Deposit, Converse County, Wyoming." *The Mountain Geologist*, Vol.11, No.2, P.85-93.
- Langmuir, Donald, 1997. *Aqueous Environmental Geochemistry*. Prentice-Hall, Inc. Upper Saddle River, New Jersey, 07458, 600 pp.

- Lewis Water Consultants, Inc., 2001. Geochemical Transport Modeling of Wellfield Restoration by Natural Attenuation.
- Manning, B.A., and Sabine Goldberg, 1997. "Adsorption and Stability of Arsenic (III) at the Clay Mineral-Water Interface." *Environmental Science and Technology*, v. 31, p. 2005-2011.
- Masscheleyn, P.H., R.D. Delaune, and W.H. Patrick, Jr., 1991. "Effect of Redox Potential and pH on Arsenic Speciation and Solubility in a Contaminated Soil." *Environmental Science and Technology*, v. 25, p. 1414-1419.
- Parkhurst, D.L., 1999. Frequently Asked Questions for PHREEQC and PhreeqcI, #86. Retrieved February 21, 2012 from [http://www.brr.cr.usgs.gov/projects/GWC\\_coupled/phreeqc/faq.html](http://www.brr.cr.usgs.gov/projects/GWC_coupled/phreeqc/faq.html) Last updated February 3, 1999.
- Parkhurst, D.L. and C.A.J. Appelo, 1999. User's Guide to PHREEQC (Version 2)—A Computer Program for Speciation, Batch-Reaction, One Dimensional Transport, and Inverse Geochemical Calculations. U.S. Geological Survey Water-Resources Investigations Report 99-425. 310 p.
- SKB, 2008. Assessment of the Radium-Barium Co-Precipitation and Its Potential Influence on the Solubility of Ra in the Near-Field. Technical Report TR-08-07. August, 52 p.
- Smedley, P. L., H. B. Nicolli, D. M. J. Macdonald, A. J. Barros, and J. O. Tullio, 2002. Hydrogeochemistry of Arsenic and Other Inorganic Constituents in Groundwaters from La Pampa, Argentina. *Applied Geochemistry* 17:259-284.
- Stewart, B., 2008. The Dominating Influence of Calcium on the Biogeochemical Fate of Uranium. PhD Dissertation. Stanford University, Stanford, California. May 2008.
- Waychunas, G.A., B.A. Rea, C.C. Fuller, and J.A. Davis, 1993. "Surface Chemistry of Ferrihydrite – Part 1 – EXAFS Studies of the Geometry of Coprecipitated and Adsorbed Arsenate." *Geochimica et Cosmochimica Acta*, v. 57, p. 2251-2269.
- Xu, M. and Y. Eckstein, 1995. "Use of Weighted Least-Squares Method in Evaluation of the Relationship Between Dispersivity and Field Scale." *Ground Water*, 33, 6: 905–908.
- Zhu, Chen, 2004. "Coprecipitation in the Barite Isostructural Family: 1. Binary Mixing Properties." *Geochimica et Cosmochimica Acta*, Vol. 68, No. 16, pp. 3327-3337.



## FIGURES



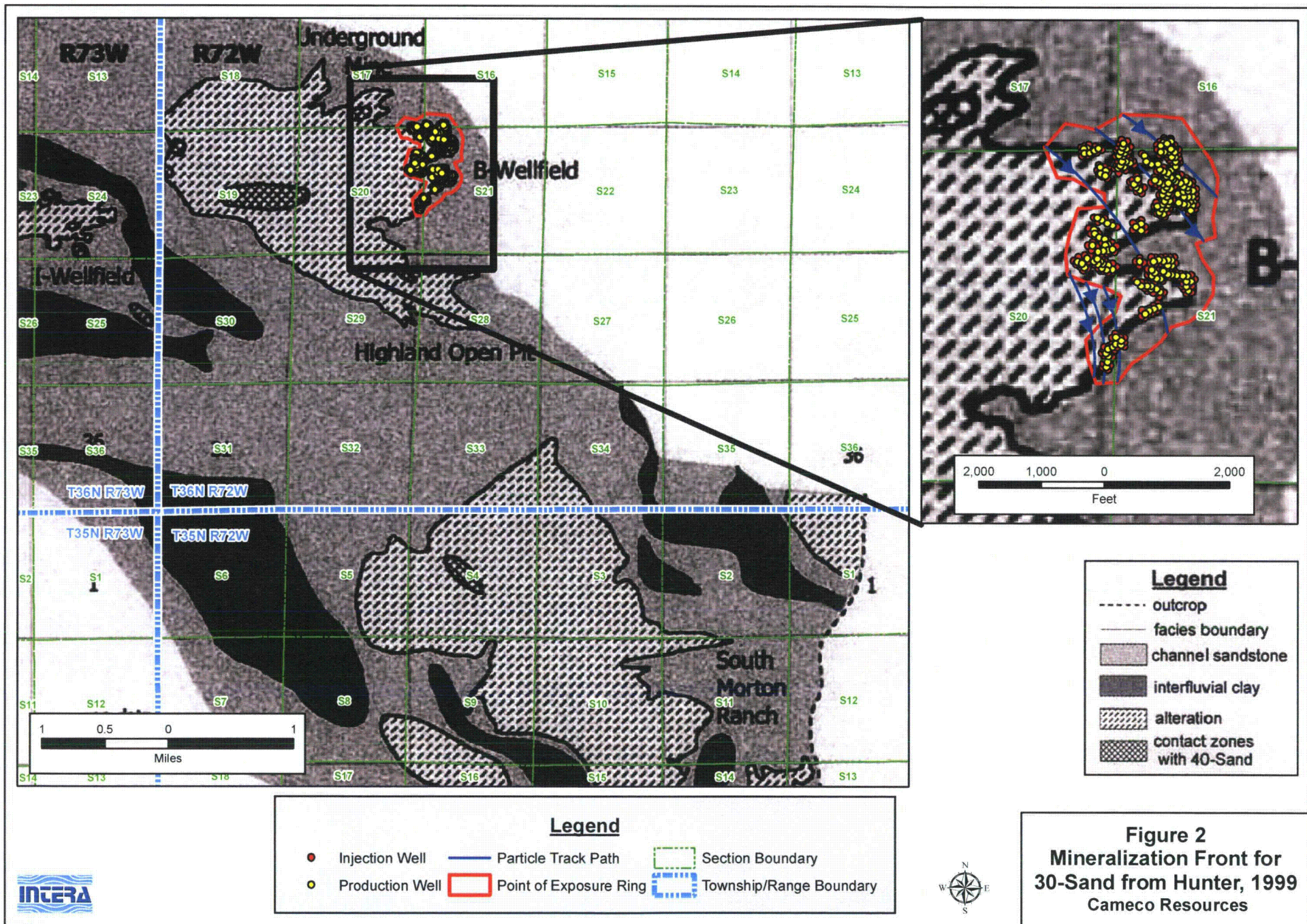


### Legend

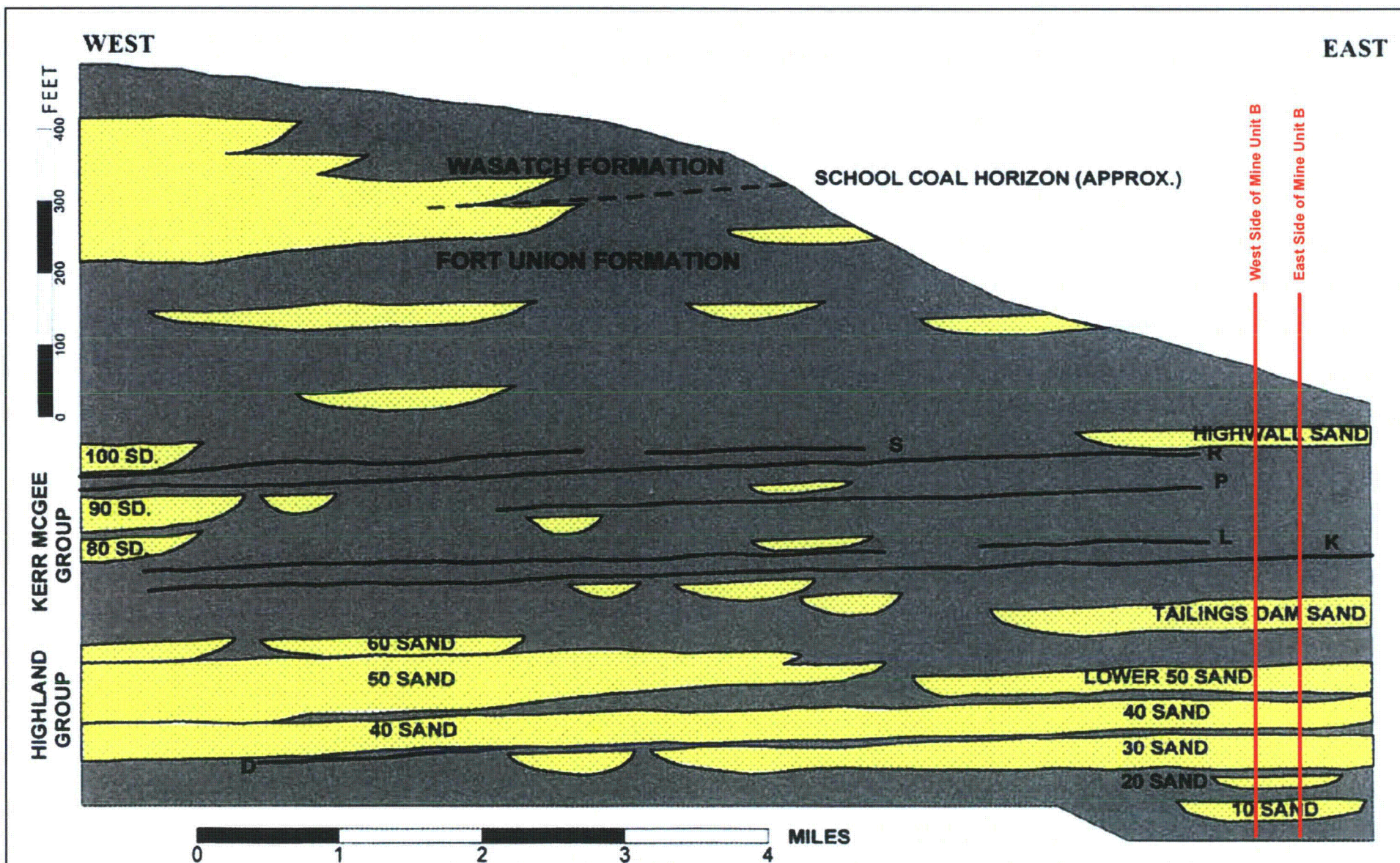
- Point of Exposure Well
- Point of Compliance Well
- Point of Exposure Ring
- Section Boundary

**Figure 1**  
**Location Map**  
**Cameco Resources**





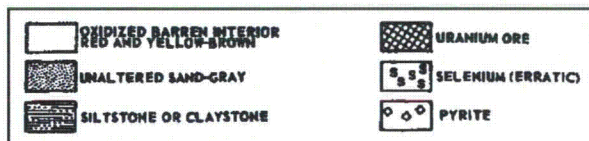
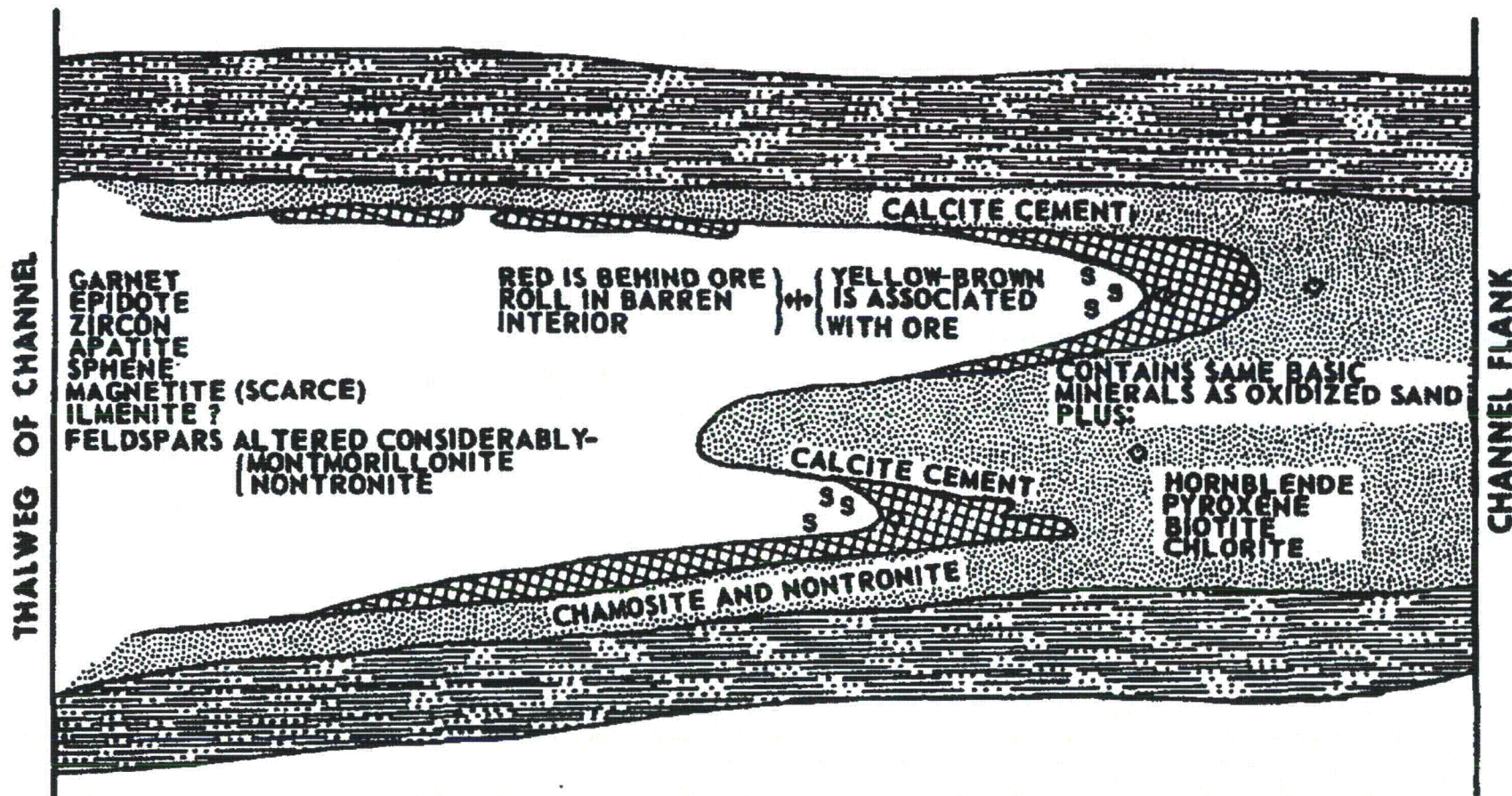




**Figure 3**  
**Modified Cross Section from Hunter, 1999**  
**Cameco Resources**



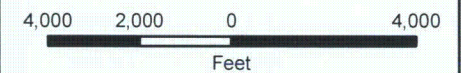




Modified from Langden and Kidwell, 1973.

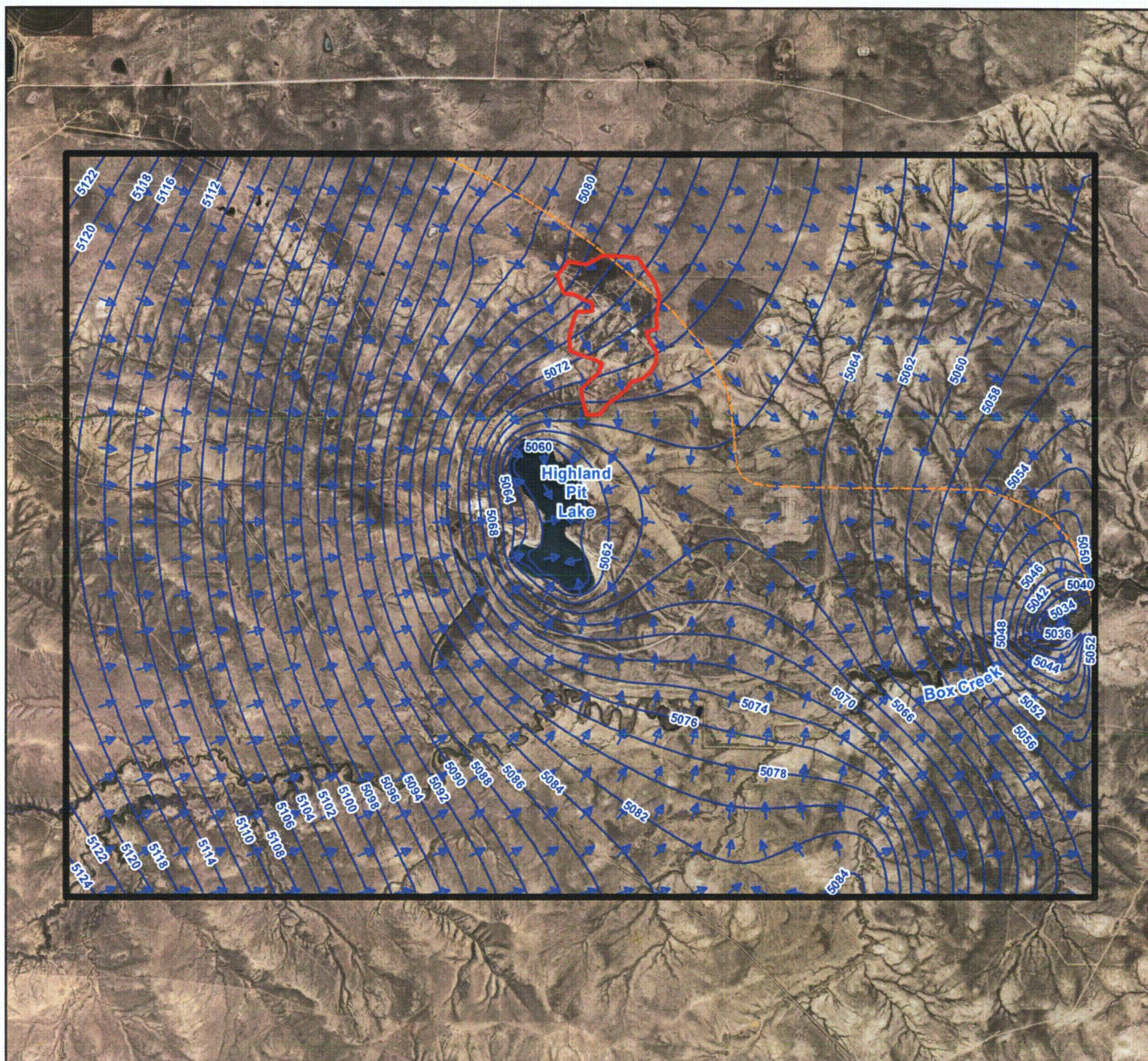
Figure 4  
Schematic Diagram of Roll-Front Deposit  
Cameco Resources





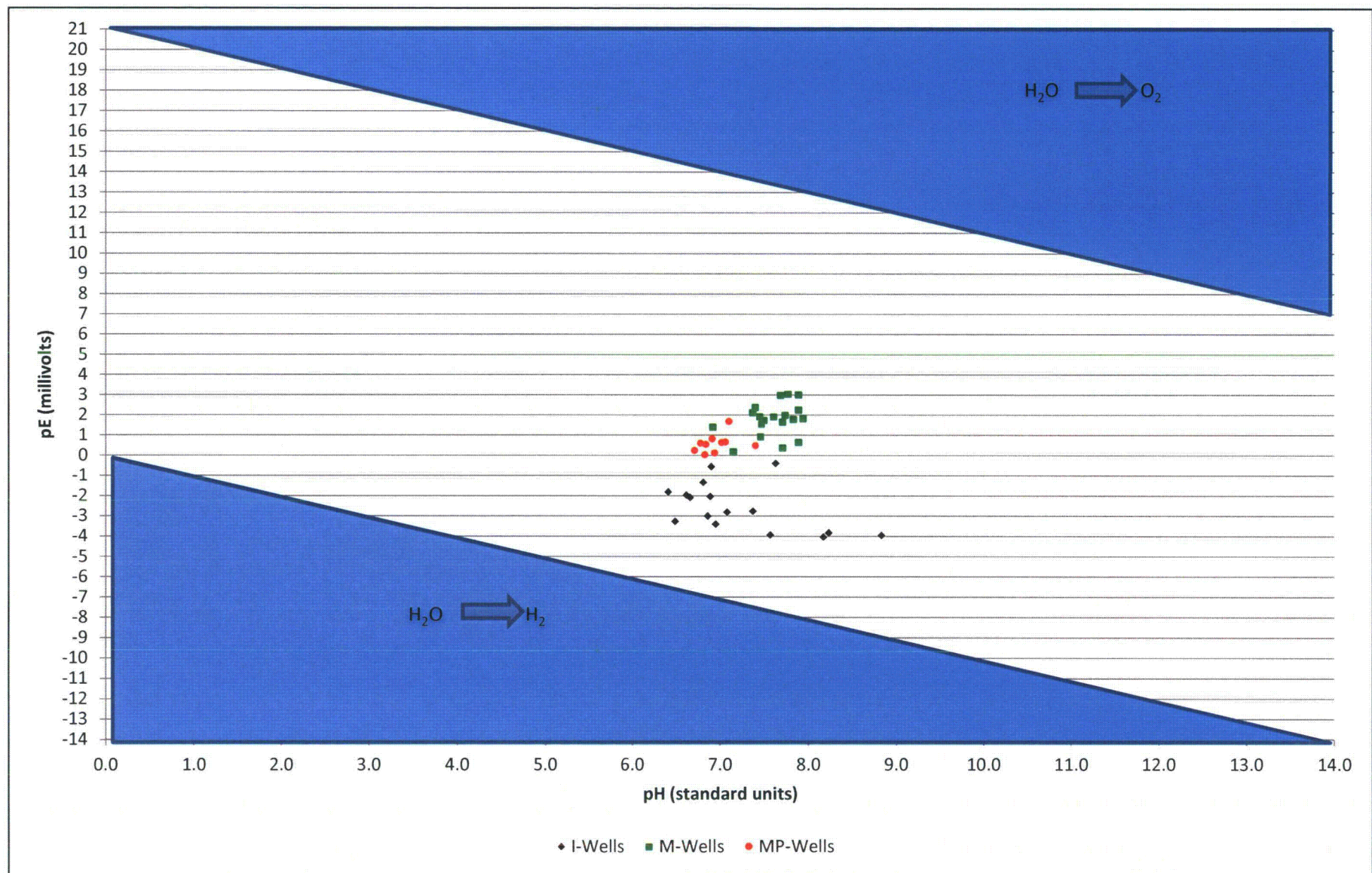
### Legend

- Groundwater Flow Direction
- Groundwater Elevation (ft-amsl)
- Groundwater Flow Divide
- Point of Exposure Ring
- Model Domain



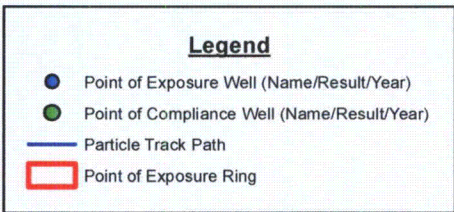
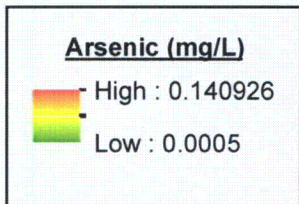
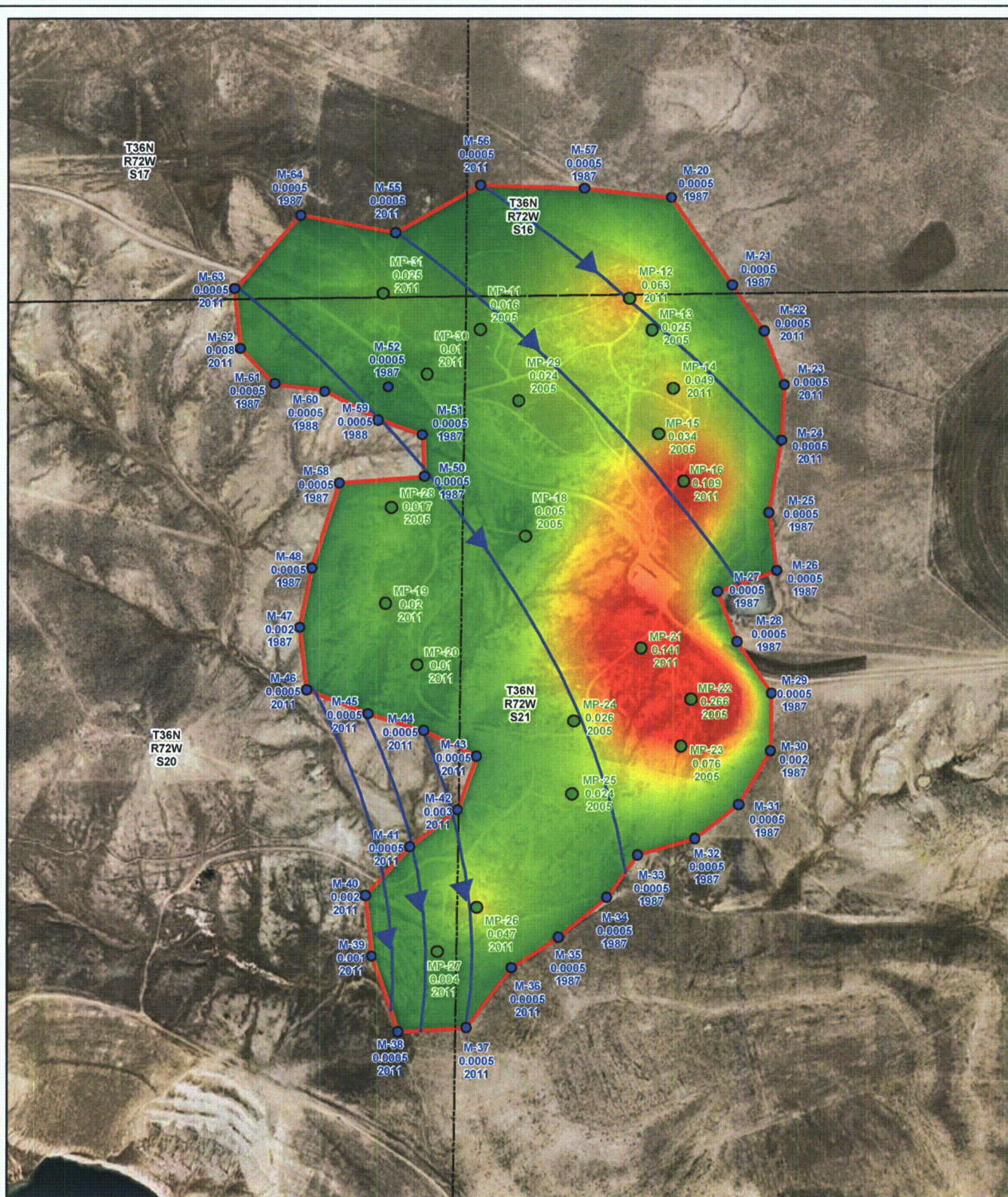
**Figure 5**  
**Projected 30-Sand**  
**Steady-State**  
**Water Level Elevation**  
**Cameco Resources**





**Figure 6**  
**pH pE Plot**  
 Cameco Resources

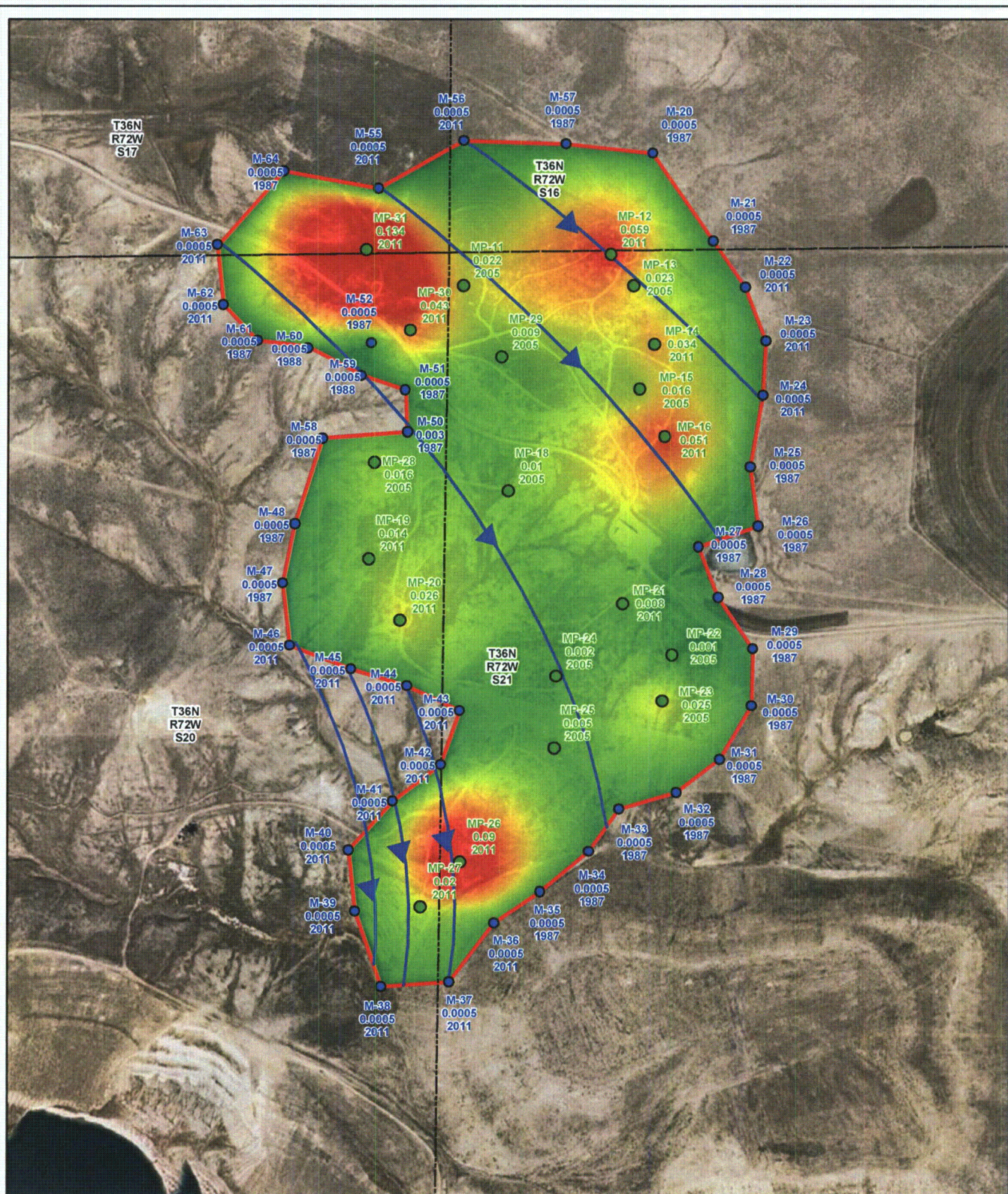




**Figure 7**  
Natural Neighbor Interpolation  
of Arsenic  
Groundwater Concentrations  
Cameco Resources







### Selenium (mg/L)

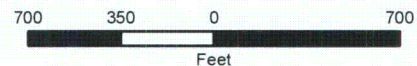


High : 0.132532

Low : 1.50454e-005

### Legend

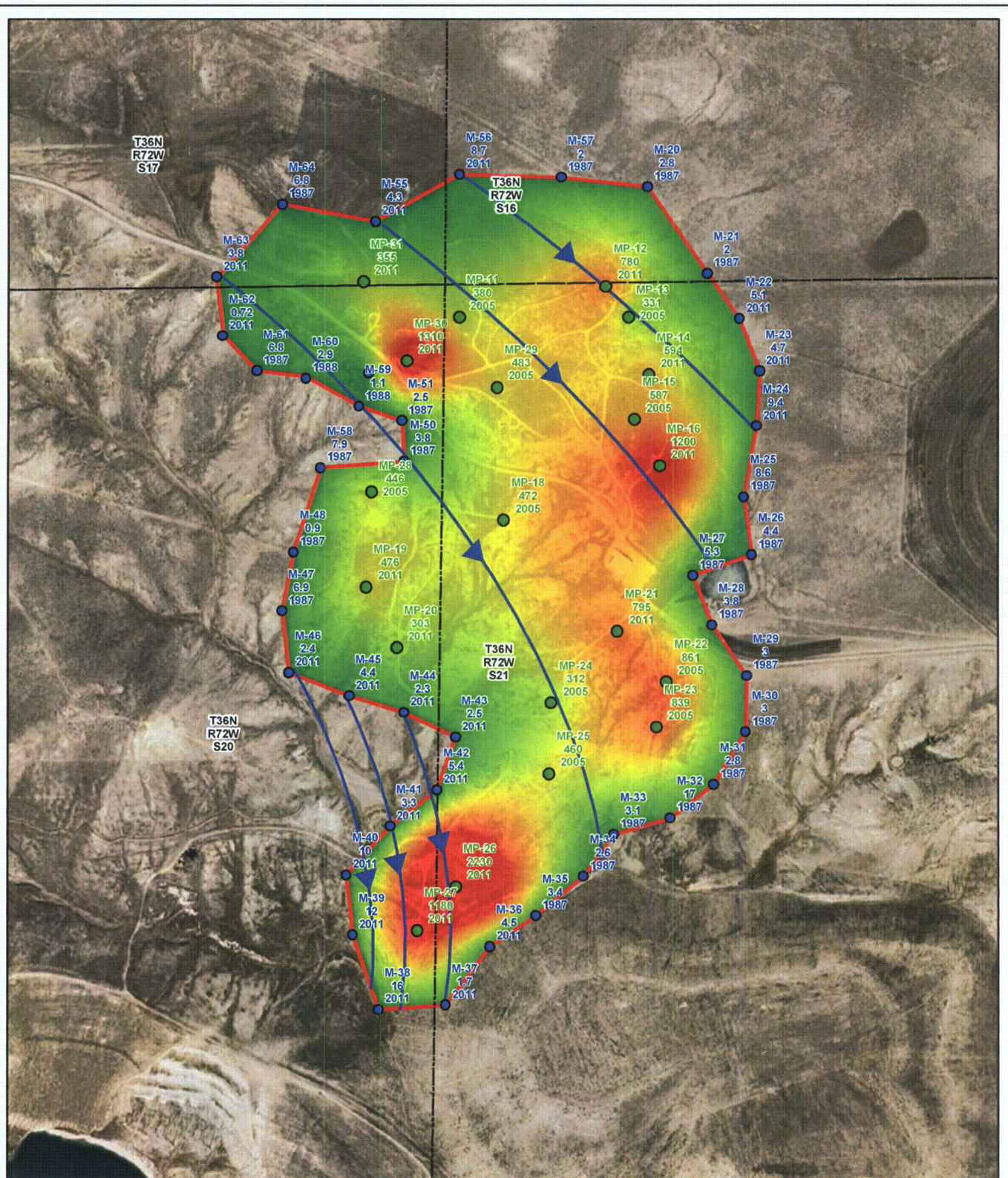
- Point of Exposure Well (Name/Result/Year)
- Point of Compliance Well (Name/Result/Year)
- Particle Track Path
- Point of Exposure Ring



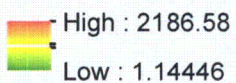
**Figure 8**  
Natural Neighbor Interpolation  
of Selenium  
Groundwater Concentrations  
Cameco Resources





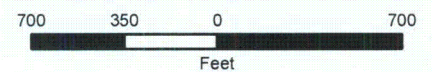


#### Radium 226 (pCi/L)



#### Legend

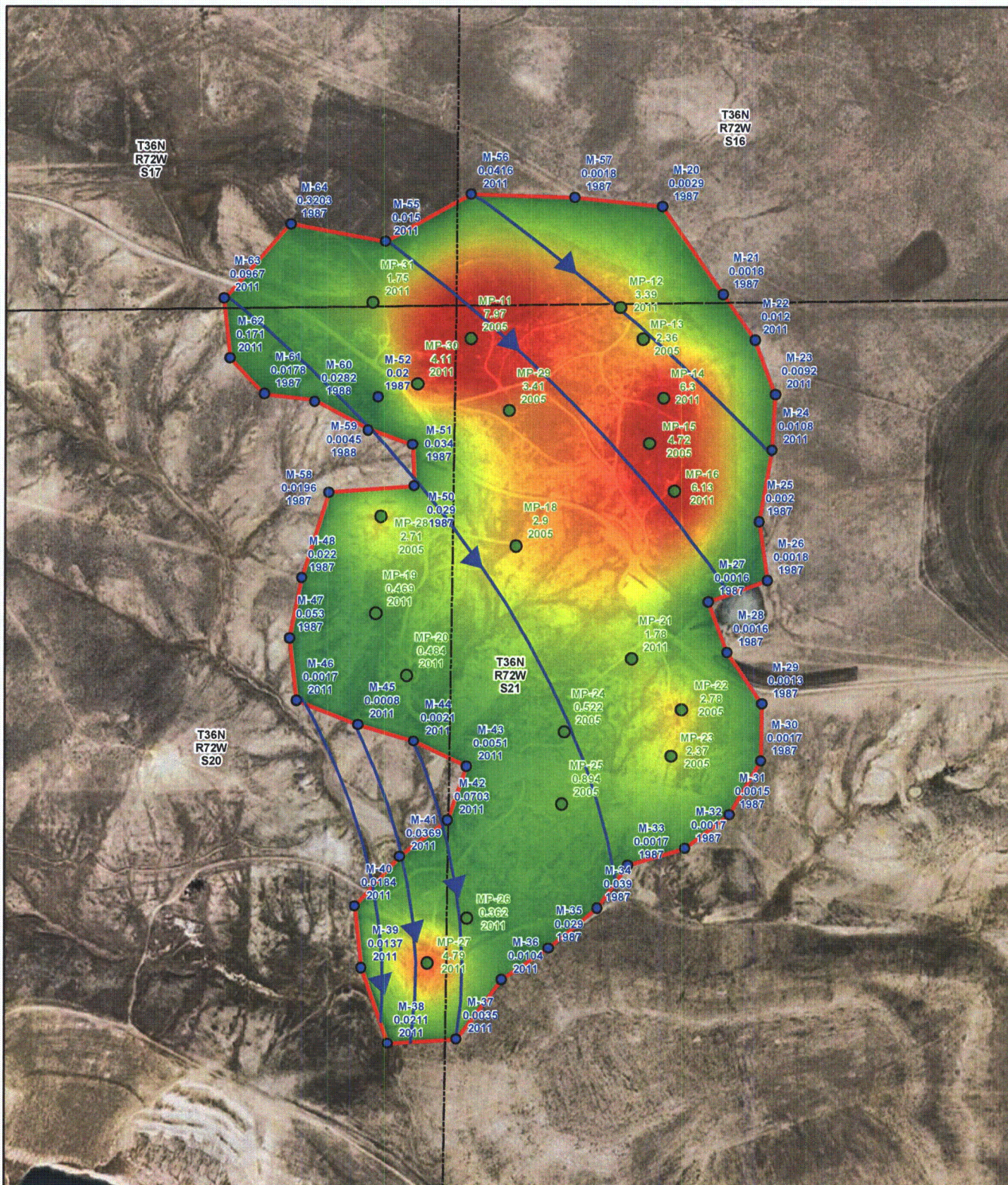
- Point of Exposure Well (Name/Result/Year)
- Point of Compliance Well (Name/Result/Year)
- Particle Track Path
- Point of Exposure Ring



**Figure 9**  
**Natural Neighbor Interpolation**  
**of Radium 226**  
**Groundwater Concentrations**  
**Cameco Resources**







#### Uranium (mg/L)

High : 7.9418  
Low : 0.00172505

#### Legend

- Point of Exposure Well (Name/Result/Year)
- Point of Compliance Well (Name/Result/Year)
- Particle Track Path
- Point of Exposure Ring

700 350 0 700  
Feet

**Figure 10**  
**Natural Neighbor Interpolation**  
**of Uranium**  
**Groundwater Concentrations**  
**Cameco Resources**





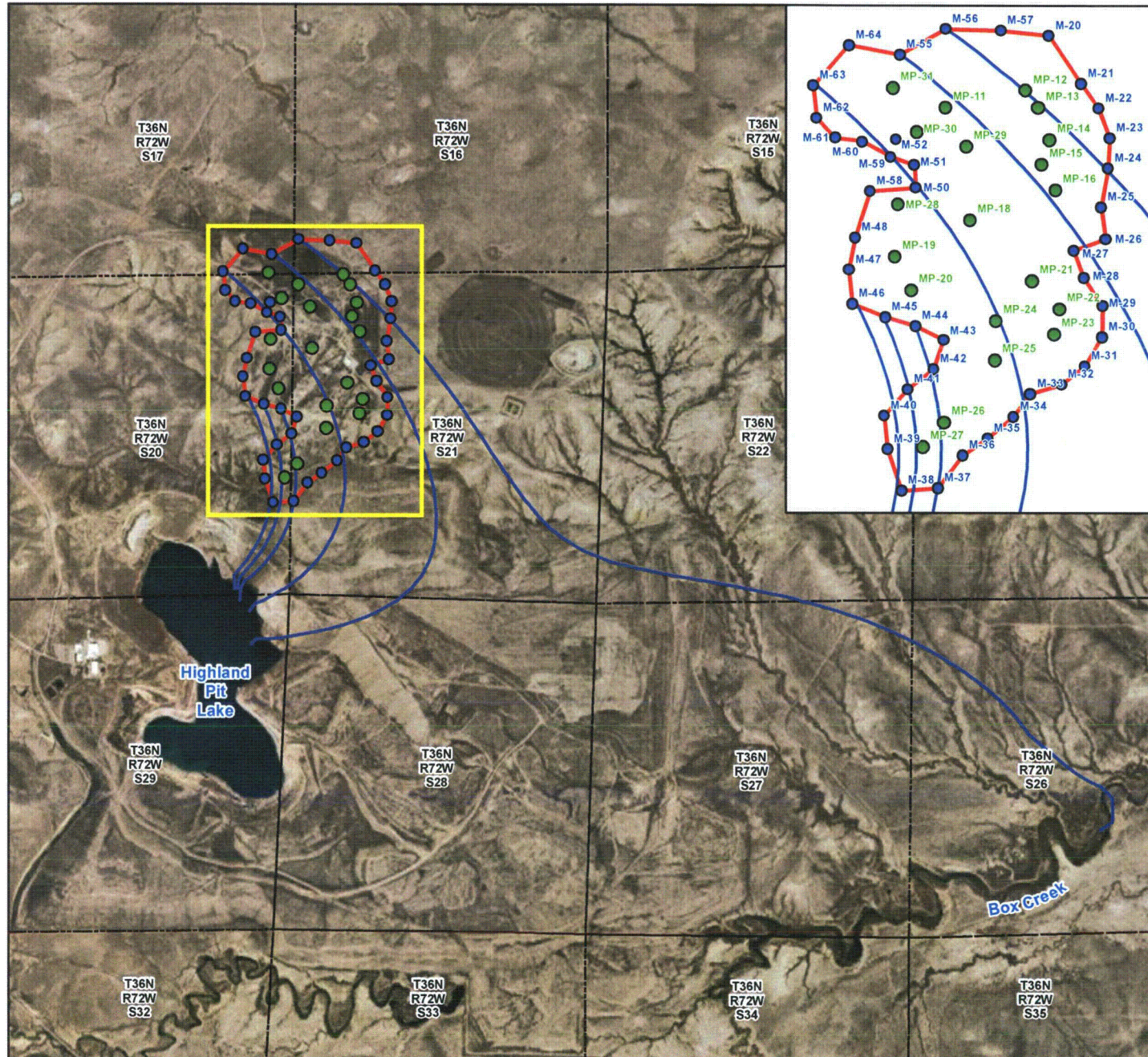


2,400 1,200 0 2,400  
Feet

### Legend

- Point of Exposure Well
- Point of Compliance Well
- Particle Track Path
- Point of Exposure Ring
- Section Boundary

**Figure 11**  
**Particle Tracks Paths**  
**Generated from**  
**Steady-State Future**  
**Condition MODFLOW**  
**Model (Aqui-Ver, 2011)**  
**Cameco Resources**



**ATTACHMENT A**  
**PHREEQC Input Files**



DATABASE C:\Program Files (x86)\USGS\Phreeqc Interactive  
2.18.5314\database\l1n1.dat  
SOLUTION 0 source solution - from Monitoring well M-44

temp	13.14	
pH	7.45	
pe	1.91	
redox	pe	
units	mg/l	
density	1	
Ca	53	
Cl	8 (charge)	0
F	0.1	
Mg	11	
Na	54	
K	6	
S(6)	109	
Fe	0.06	
Mn	0.02	
Se	0.0005	
U	0.0021	
Ra	2.3e-009	
Ba	0.02	
As	0.0005	
C(4)	207	
N(-3)	0.12	
-water	1 # kg	

SOLUTION 1-4 Downgradient from Monitoring well M-44

temp	13.14	
pH	7.45	
pe	1.91	
redox	pe	
units	mg/l	
density	1	
Ca	53	
Cl	8 (charge)	0
F	0.1	
Mg	11	
Na	54	
K	6	
S(6)	109	
Fe	0.06	
Mn	0.02	
Se	0.0005	
U	0.0021	
Ra	2.3e-009	
Ba	0.02	
As	0.0005	
C(4)	207	
N(-3)	0.12	
-water	1 # kg	

SOLUTION 5-6 Production Zone - MP-26

temp	10.63
pH	7.1
pe	1.67
redox	pe
units	mg/l
density	1
Ca	43.3
Cl	3 (charge) 0
F	0.05
Mg	8.2
Na	6.6
K	6.2
S(6)	5
Fe	19
Mn	0.61
Se	0.09
U	0.362
Ra	2.23e-006
Ba	0.02
As	0.047
C(4)	205
N(-3)	4.58
-water	1 # kg

SOLUTION 7-9 Downgradient Monitoring Well M-37

temp	12.26
pH	7.89
pe	2.23
redox	pe
units	mg/l
density	1
Ca	39
Cl	3 (charge) 0
F	0.2
Mg	7
Na	59
K	5
S(6)	98
Fe	0.78
Mn	0.06
Se	0.0005
U	0.0035
Ra	1.7e-009
Ba	0.02
As	0.0005
C(4)	179
N(-3)	1.21
-water	1 # kg

EQUILIBRIUM\_PHASES 1-5 #upgradient/oxidized  
quartz 0 1

```

k-feldspar 0 .5
montmor-k 0 .2
hematite 0 .5
EQUILIBRIUM_PHASES 6 #transition zone/mine area
uraninite 0 .1
coffinite 0 .1
quartz 0 1
k-feldspar 0 .5
siderite 0 0
montmor-k 0 .2
EQUILIBRIUM_PHASES 7-9 #downgradient/reduced w/ hfo
goethite 0 .01
quartz 0 1
k-feldspar 0 .5
Pyrite 0 1.2
montmor-k 0 .2
Uraninite 0 0
Coffinite 0 0
Calcite 0 0
Ferroselite 0 0
Siderite 0 0
gypsum 0 0
Se 0 0
RaSO4 0 0
Barite 0 0
SOLUTION_SPECIES
1.0000 H2AsO4- + 1.0000 F- = AsO3F-- +1.0000 H2O
    -llnl_gamma 4.0
    log_k -40
1.0000 H2AsO4- + 1.0000 H+ + 1.0000 F- = HAsO3F- +1.0000 H2O
    -llnl_gamma 4.0
    log_k -46
EXCHANGE_SPECIES
Ra+2 + 2X- = RaX2
    log_k 0.91
    delta_h 4.5 kJ
    -gamma 5 0
SURFACE_SPECIES
Hfo_wOH + CO3-2 + H+ = Hfo_wOCO2- + H2O
    log_k = 12.78

Hfo_wOH + CO3-2 + 2H+ = Hfo_wOCO2H + H2O
    log_k = 20.37

Hfo_wOH + As(OH)3 = Hfo_wH2AsO3 + H2O
    log_k 5.41
AsO4-3 + 3H+ + Hfo_wOH = Hfo_wH2AsO4 + H2O
    log_k 29.31
AsO4-3 + 2H+ + Hfo_wOH = Hfo_wHAsO4- + H2O
    log_k 23.51
AsO4-3 + Hfo_wOH = Hfo_wOHasO4-3

```



```

    log_k      10.58
Hfo_wOH + Ra+2 = Hfo_wORa+ + H+
    log_k      -3.5
H2O + Hfo_wOH + Ra+2 = Hfo_wORaOH + 2H+
    log_k      -12.95
Ca+2 + Hfo_wOH = Hfo_wOCa+ + H+
    log_k      -5
Ca+2 + H2O + Hfo_wOH = Hfo_wOCaOH + 2H+
    log_k      -14.5
END
EXCHANGE 1-6
    X          0.7
    -equilibrate with solution 1
    #-pitzer_exchange_gammas true
EXCHANGE 7-9
    X          0.7
    -equilibrate with solution 7
    #-pitzer_exchange_gammas true
END
SURFACE 7
    #-equilibrate with solution 7
    Hfo_wOH Goethite      equilibrium_phase 0.2      53300
    Hfo_sOH Goethite      equilibrium_phase 0.005
END

SOLID_SOLUTIONS 7-9
    Ba(x)Ra(1-x)SO4
        -comp Barite 0
        -comp RaSO4 0
END

TRANSPORT
    -cells          9
    -shifts         61
    -time_step      523819419 # seconds
    -initial_time   0
    -boundary_conditions constant flux
    -lengths        9*50
    -dispersivities 9*8.9
    -punch_cells    9
    -punch_frequency 1
    -multi_d        false

USER_GRAPH
    -headings Years U Se As Mn Fe SO4 Ra(pCi/L) RaX2 pe pH
    -chart_title "GW Solute Concentrations at POE (M-44 -> M-37)"
    -axis_titles "(Years)" "Milligrams per Liter" "pe / pH"
    -axis_scale x_axis 0 1000 500
    -axis_scale y_axis 1e-13 1500 auto auto log scale
    -axis_scale sy_axis -14 21 3
    -initial_solutions false

```

```
-plot_concentration_vs TOTAL_TIME
-start
10 GRAPH_X TOTAL_TIME/31556926
20 GRAPH_Y TOT("U")*238029, TOT("Se")*78960, TOT("As")*74922,
TOT("Mn")*54938, TOT("Fe")*55845, TOT("S(6)")*32065, TOT("Ra")*226000*1e9,
MOL("RaX2"), #SURF("Ra","Hfo")
#Multipliers after each variable are to convert to mg/L from Molality,
then to pCi/L for Ra
30 GRAPH_SY LOG10(ACT("e-"))*-1, LOG10(ACT("H+"))*-1
-end
END
```

DATABASE C:\Program Files (x86)\USGS\Phreeqc Interactive  
2.18.5314\database\llnl.dat  
SOLUTION 0 source solution - from Monitoring well M-45

temp	13.22	
pH	7.71	
pe	1.64	
redox	pe	
units	mg/l	
density	1	
Ca	45	
Cl	3 (charge)	0
F	0.2	
Mg	9	
Na	52	
K	6	
S(6)	93	
Fe	4.44	
Mn	0.07	
Se	0.0005	
U	0.0104	
Ra	4.4e-009	
Ba	0.02	
As	0.006	
C(4)	199	
N(-3)	2.12	
-water	1 # kg	

SOLUTION 1-4 Downgradient from Monitoring well M-45

temp	13.22	
pH	7.71	
pe	1.64	
redox	pe	
units	mg/l	
density	1	
Ca	45	
Cl	3 (charge)	0
F	0.2	
Mg	9	
Na	52	
K	6	
S(6)	93	
Fe	4.44	
Mn	0.07	
Se	0.0005	
U	0.0104	
Ra	4.4e-009	
Ba	0.02	
As	0.006	
C(4)	199	
N(-3)	2.12	
-water	1 # kg	

SOLUTION 5-6 Production Zone - MP-27

temp	13.15
pH	6.83
pe	.019
redox	pe
units	mg/l
density	1
Ca	116
Cl	5 (charge) 0
F	0.05
Mg	23
Na	22
K	7
S(6)	34
Fe	.8
Mn	0.41
Se	0.02
U	4.79
Ra	1.18e-006
Ba	0.02
As	0.004
C(4)	482
N(-3)	.12
-water	1 # kg

SOLUTION 7-9 Downgradient Monitoring Well M-38

temp	14.94
pH	7.61
pe	1.89
redox	pe
units	mg/l
density	1
Ca	54
Cl	5 (charge) 0
F	0.2
Mg	10
Na	56
K	6
S(6)	102
Fe	0.42
Mn	0.05
Se	0.0005
U	0.0211
Ra	1.6e-8
Ba	0.02
As	0.0005
C(4)	211
N(-3)	.27
-water	1 # kg

EQUILIBRIUM\_PHASES 1-4 #upgradient/oxidized  
quartz 0 1

```

k-feldspar 0 .5
montmor-k 0 .2
EQUILIBRIUM_PHASES 5-6 #transition zone/mine area
uraninite 0 .1
coffinite 0 .1
quartz 0 1
k-feldspar 0 .5
siderite 0 0
montmor-k 0 .2
EQUILIBRIUM_PHASES 7-9 #downgradient/reduced w/ hfo
goethite 0 .01
quartz 0 1
k-feldspar 0 .5
Pyrite 0 1.2
montmor-k 0 .2
Uraninite 0 0
Coffinite 0 0
Calcite 0 0
Ferroselite 0 0
Siderite 0 0
gypsum 0 0
Se 0 0
RaSO4 0 0
Barite 0 0
SOLUTION_SPECIES
1.0000 H2AsO4- + 1.0000 F- = AsO3F-- +1.0000 H2O
    -llnl_gamma 4.0
    log_k -40
1.0000 H2AsO4- + 1.0000 H+ + 1.0000 F- = HAsO3F- +1.0000 H2O
    -llnl_gamma 4.0
    log_k -46
EXCHANGE_SPECIES
Ra+2 + 2X- = RaX2
    log_k 0.91
    delta_h 4.5 kJ
    -gamma 5 0
SURFACE_SPECIES
Hfo_wOH + CO3-2 + H+ = Hfo_wOCO2- + H2O
    log_k = 12.78

Hfo_wOH + CO3-2 + 2H+ = Hfo_wOCO2H + H2O
    log_k = 20.37

Hfo_wOH + As(OH)3 = Hfo_wH2AsO3 + H2O
    log_k 5.41
AsO4-3 + 3H+ + Hfo_wOH = Hfo_wH2AsO4 + H2O
    log_k 29.31
AsO4-3 + 2H+ + Hfo_wOH = Hfo_wHAsO4- + H2O
    log_k 23.51
AsO4-3 + Hfo_wOH = Hfo_wOHasO4-3
    log_k 10.58

```

```

Hfo_wOH + Ra+2 = Hfo_wORa+ + H+
  log_k      -3.5
H2O + Hfo_wOH + Ra+2 = Hfo_wORaOH + 2H+
  log_k      -12.95
Ca+2 + Hfo_wOH = Hfo_wOCa+ + H+
  log_k      -5
Ca+2 + H2O + Hfo_wOH = Hfo_wOCaOH + 2H+
  log_k      -14.5
END
EXCHANGE 1-6
  X          0.7
  -equilibrate with solution 1
  #-pitzer_exchange_gammas true
EXCHANGE 7-9
  X          0.7
  -equilibrate with solution 7
  #-pitzer_exchange_gammas true
SURFACE 7
  #-equilibrate with solution 7
  Hfo_wOH Goethite      equilibrium_phase 0.2      53300
  Hfo_sOH Goethite      equilibrium_phase 0.005
END

SOLID_SOLUTIONS 7-9
  Ba(x)Ra(1-x)SO4
    -comp Barite 0
    -comp RaSO4 0
END

TRANSPORT
  -cells          9
  -shifts         61
  -time_step      523819419 # seconds
  -initial_time   0
  -boundary_conditions constant flux
  -lengths        9*50
  -dispersivities 9*8.9
  -punch_cells    9
  -punch_frequency 1
  -multi_d        false

USER_GRAPH
  -headings Years U Se As Mn Fe SO4 Ra(pCi/L) RaX2 pe pH
  -chart_title "GW Solute Concentrations at POE (M-45 -> M-38)"
  -axis_titles "(Years)" "Milligrams per Liter" "pe / pH"
  -axis_scale x_axis 0 1000 500
  -axis_scale y_axis 1e-13 1500 auto auto log scale
  -axis_scale sy_axis -14 21 3
  -initial_solutions false
  -plot_concentration_vs TOTAL_TIME
  -start

```

```
10 GRAPH_X TOTAL_TIME/31556926
20 GRAPH_Y TOT("U")*238029, TOT("Se")*78960, TOT("As")*74922,
TOT("Mn")*54938, TOT("Fe")*55845, TOT("S(6)")*32065, TOT("Ra")*226000*1e9,
MOL("RaX2"), #SURF("Ra","Hfo")
#Multipliers after each variable are to convert to mg/L from Molality,
then to pCi/L for Ra
30 GRAPH_SY LOG10(ACT("e-"))*-1, LOG10(ACT("H+"))*-1
-end
END
```

DATABASE C:\Program Files (x86)\USGS\Phreeqc Interactive  
2.18.5314\database\llnl.dat  
SOLUTION 0 source solution - from Monitoring well M-55

temp	13.72
pH	7.69
pe	2.97
redox	pe
units	mg/l
density	1
Ca	43
Cl	4 (charge) 0
F	0.2
Mg	10
Na	58
K	5
S(6)	91
Fe	0.96
Mn	0.04
Se	0.0005
U	0.015
Ra	4.3e-009
Ba	0.02
As	0.0005
C(4)	210
N(-3)	0.2
-water	1 # kg

SOLUTION 1-2 source solution - from Monitoring well M-55

temp	13.72
pH	7.69
pe	2.97
redox	pe
units	mg/l
density	1
Ca	43
Cl	4 (charge) 0
F	0.2
Mg	10
Na	58
K	5
S(6)	91
Fe	0.96
Mn	0.04
Se	0.0005
U	0.015
Ra	4.3e-009
Ba	0.02
As	0.0005
C(4)	210
N(-3)	0.2
-water	1 # kg



SOLUTION 3-14 Production Zone - MP-16

temp	13.48
pH	6.71
pe	0.24
redox	pe
units	mg/l
density	1
Ca	76
Cl	7 (charge) 0
F	0.05
Mg	15
Na	47
K	6
S(6)	27
Fe	3.48
Mn	0.34
Se	0.051
U	6.13
Ra	1.2e-006
Ba	0.02
As	0.109
C(4)	376
N(-3)	0.23
-water	1 # kg

SOLUTION 15-16 Downgradient Monitoring Well M-24

temp	12.45
pH	7.83
pe	1.76
redox	pe
units	mg/l
density	1
Ca	44
Cl	3 (charge) 0
F	0.2
Mg	10
Na	53
K	6
S(6)	88
Fe	0.65
Mn	0.03
Se	0.0005
U	0.0108
Ra	9.4e-009
Ba	0.02
As	0.0005
C(4)	195
N(-3)	0.22
-water	1 # kg

EQUILIBRIUM\_PHASES 1-2 #downgradient/reduced  
quartz 0 1

```

k-feldspar 0 .5
Pyrite      0 1.2
montmor-k   0 .2
Uraninite   0 0
Coffinite   0 0
Calcite      0 0
Ferroselite 0 0
Siderite     0 0
gypsum       0 0
Se           0 0
RaSO4        0 0
Barite       0 0
EQUILIBRIUM_PHASES 3-14 #transition zone/mine area
goethite     0 .01
uraninite    0 .1
coffinite    0 .1
quartz       0 1
k-feldspar   0 .5
siderite     0 0
montmor-k    0 .2
EQUILIBRIUM_PHASES 15-16 #downgradient/reduced w/ hfo
quartz       0 1
k-feldspar   0 .5
Pyrite      0 1.2
montmor-k    0 .2
Uraninite    0 0
Coffinite    0 0
Calcite      0 0
Ferroselite  0 0
Siderite     0 0
gypsum       0 0
Se           0 0
RaSO4        0 0
Barite       0 0
SOLUTION_SPECIES
1.0000 H2AsO4- + 1.0000 F- = AsO3F-- +1.0000 H2O
      -llnl_gamma          4.0
      log_k                 -40
1.0000 H2AsO4- + 1.0000 H+ + 1.0000 F- = HAsO3F- +1.0000 H2O
      -llnl_gamma          4.0
      log_k                 -46
EXCHANGE_SPECIES
Ra+2 + 2X- = RaX2
      log_k          0.91
      delta_h        4.5 kJ
      -gamma         5 0
SURFACE_SPECIES
Hfo_wOH + CO3-2 + H+ = Hfo_wOCO2- + H2O
      log_k = 12.78

Hfo_wOH + CO3-2 + 2H+ = Hfo_wOCO2H + H2O

```

```

log_k = 20.37

Hfo_WOH + As(OH)3 = Hfo_WH2AsO3 + H2O
log_k 5.41
AsO4-3 + 3H+ + Hfo_WOH = Hfo_WH2AsO4 + H2O
log_k 29.31
AsO4-3 + 2H+ + Hfo_WOH = Hfo_WHAsO4- + H2O
log_k 23.51
AsO4-3 + Hfo_WOH = Hfo_WOHAsO4-3
log_k 10.58
Hfo_WOH + Ra+2 = Hfo_WORa+ + H+
log_k -3.5
H2O + Hfo_WOH + Ra+2 = Hfo_WORaOH + 2H+
log_k -12.95
Ca+2 + Hfo_WOH = Hfo_WOCa+ + H+
log_k -5
Ca+2 + H2O + Hfo_WOH = Hfo_WOCaOH + 2H+
log_k -14.5
END
EXCHANGE 1-2
X 0.7
-equilibrate with solution 1
-pitzer_exchange_gammas true
EXCHANGE 3-14
X 0.7
-equilibrate with solution 3
-pitzer_exchange_gammas true
EXCHANGE 15-16
X 0.7
-equilibrate with solution 15
-pitzer_exchange_gammas true
SURFACE 3-14
#-equilibrate with solution 15
Hfo_WOH Goethite equilibrium_phase 0.2 53300
Hfo_SOH Goethite equilibrium_phase 0.005
END
SOLID_SOLUTIONS 15-16
Ba(x)Ra(1-x)SO4
-comp Barite 0
-comp RaSO4 0
END

TRANSPORT
-cells 16
-shifts 65
-initial_time 0
-time_step 993346615 # seconds
-boundary_conditions constant flux
-lengths 16*50
-dispersivities 16*10.7
-punch_frequency 1

```

```
-punch_cells      16
-multi_d          false
```

USER\_GRAPH

```
-headings Years U Se As Mn Fe SO4 Ra(pCi/L) RaX2 pE pH
-chart_title "GW Solute Concentrations at POE (M55 -> M-24)"
-axis_titles "(Years)" "Milligrams per Liter" "pE / pH"
-axis_scale x_axis 0 1000 500
-axis_scale y_axis 1e-12 1500 auto auto log scale
-axis_scale sy_axis -14 21 3
-initial_solutions false
-plot_concentration_vs TOTAL_TIME
-start
10 GRAPH_X TOTAL_TIME/31556926
20 GRAPH_Y TOT("U")*238029, TOT("Se")*78960, TOT("As")*74922,
TOT("Mn")*54938, TOT("Fe")*55845, TOT("S(6)")*32065, TOT("Ra")*226000*1e9,
MOL("RaX2"), #SURF("Ra","Hfo")
#Multipliers after each variable are to convert to mg/L from Molality,
then to pCi/L for Ra
30 GRAPH_SY LOG10(ACT("e-"))*-1, LOG10(ACT("H+"))*-1
-end
END
```



DATABASE C:\Program Files (x86)\USGS\Phreeqc Interactive  
2.18.5314\database\llnl.dat  
SOLUTION 0 source solution - from Monitoring well M-56

temp	13.82	
pH	7.47	
pe	1.54	
redox	pe	
units	mg/l	
density	1	
Ca	133	
Cl	10 (charge)	0
F	0.1	
Mg	29	
Na	90	
K	9	
S(6)	433	
Fe	0.91	
Mn	0.08	
Se	0.0005	
U	0.0416	
Ra	8.7e-009	
Ba	0.02	
As	0.0005	
C(4)	226	
N(-3)	0.45	
-water	1 # kg	

SOLUTION 1-4 source solution - from Monitoring well M-56

temp	13.82	
pH	7.47	
pe	1.54	
redox	pe	
units	mg/l	
density	1	
Ca	133	
Cl	10 (charge)	0
F	0.1	
Mg	29	
Na	90	
K	9	
S(6)	433	
Fe	0.91	
Mn	0.08	
Se	0.0005	
U	0.0416	
Ra	8.7e-009	
Ba	0.02	
As	0.0005	
C(4)	226	
N(-3)	0.45	
-water	1 # kg	

SOLUTION 5-7 Production Zone - MP-12

temp	15.09
pH	6.91
pe	0.81
redox	pe
units	mg/l
density	1
Ca	67
Cl	9 (charge) 0
F	0.2
Mg	14
Na	36
K	6
S(6)	51
Fe	4.48
Mn	0.39
Se	0.059
U	3.39
Ra	7.8e-007
Ba	0.02
As	0.063
C(4)	287
N(-3)	3.87
-water	1 # kg

SOLUTION 8-12 Downgradient Monitoring Well M-24

temp	12.45
pH	7.83
pe	1.76
redox	pe
units	mg/l
density	1
Ca	44
Cl	3 (charge) 0
F	0.2
Mg	10
Na	53
K	6
S(6)	88
Fe	0.65
Mn	0.03
Se	0.0005
U	0.0108
Ra	9.4e-009
Ba	0.02
As	0.0005
C(4)	195
N(-3)	0.22
-water	1 # kg

EQUILIBRIUM\_PHASES 1-4 #downgradient/reduced  
quartz 0 1

```

k-feldspar 0 .5
Pyrite      0 1.2
montmor-k   0 .2
Uraninite   0 0
Coffinite   0 0
Calcite      0 0
Ferroselite 0 0
Siderite     0 0
gypsum       0 0
Se           0 0
RaSO4        0 0
Barite       0 0
EQUILIBRIUM_PHASES 5-7 #transition zone/mine area
hematite     0 .5
goethite     0 .01
uraninite    0 .1
coffinite    0 .1
quartz       0 1
k-feldspar   0 .5
siderite     0 0
montmor-k    0 .2
orpiment     0 0
realgar      0 0
EQUILIBRIUM_PHASES 8-12 #downgradient/reduced w/ hfo
quartz       0 1
k-feldspar   0 .5
Pyrite       0 1.2
montmor-k    0 .2
Uraninite    0 0
Coffinite    0 0
Calcite      0 0
Ferroselite  0 0
Siderite     0 0
gypsum       0 0
Se           0 0
RaSO4        0 0
Barite       0 0
orpiment     0 0
realgar      0 0
SOLUTION_SPECIES
1.0000 H2AsO4- + 1.0000 F- = AsO3F-- +1.0000 H2O
      -llnl_gamma          4.0
      log_k                 -40
1.0000 H2AsO4- + 1.0000 H+ + 1.0000 F- = HAsO3F- +1.0000 H2O
      -llnl_gamma          4.0
      log_k                 -46
EXCHANGE_SPECIES
Ra+2 + 2X- = RaX2
      log_k          0.91
      delta_h        4.5 kJ
      -gamma         5 0

```



SURFACE\_SPECIES

Hfo\_wOH + CO3-2 + H+ = Hfo\_wOCO2- + H2O  
 $\log_k = 12.78$

Hfo\_wOH + CO3-2 + 2H+ = Hfo\_wOCO2H + H2O  
 $\log_k = 20.37$

Hfo\_wOH + As(OH)3 = Hfo\_wH2AsO3 + H2O  
 $\log_k = 5.41$

AsO4-3 + 3H+ + Hfo\_wOH = Hfo\_wH2AsO4 + H2O  
 $\log_k = 29.31$

AsO4-3 + 2H+ + Hfo\_wOH = Hfo\_wHAsO4- + H2O  
 $\log_k = 23.51$

AsO4-3 + Hfo\_wOH = Hfo\_wOHasO4-3  
 $\log_k = 10.58$

Hfo\_wOH + Ra+2 = Hfo\_wORa+ + H+  
 $\log_k = -3.5$

H2O + Hfo\_wOH + Ra+2 = Hfo\_wORaOH + 2H+  
 $\log_k = -12.95$

Ca+2 + Hfo\_wOH = Hfo\_wOCa+ + H+  
 $\log_k = -5$

Ca+2 + H2O + Hfo\_wOH = Hfo\_wOCaOH + 2H+  
 $\log_k = -14.5$

END

#EXCHANGE 1-4

#X 0.7

#-equilibrate with solution 1

#-pitzer\_exchange\_gammas true

EXCHANGE 5-7

X 0.7

-equilibrate with solution 5

#-pitzer\_exchange\_gammas true

EXCHANGE 8-12

X 0.7

-equilibrate with solution 8

#-pitzer\_exchange\_gammas true

END

SURFACE 5-7

#-equilibrate 5-7

Hfo\_wOH Goethite equilibrium\_phase 0.2 53300

Hfo\_sOH Goethite equilibrium\_phase 0.005

END

SOLID\_SOLUTIONS 8-12

Ba(x)Ra(1-x)SO4

-comp Barite 0

-comp RaSO4 0

END

TRANSPORT

```
-cells 12
-shifts 52
-time_step 607433787 # seconds
-boundary_conditions constant flux
-lengths 12*50
-dispersivities 12*9.8
-punch_cells 12
-punch_frequency 1
-multi_d false
```

USER\_GRAPH

```
-headings Years U Se As Mn Fe SO4 Ra(pCi/L) RaX2 pe pH
-chart_title "GW Solute Concentrations at POE (M56 -> M-24)"
-axis_titles "(Years)" "Milligrams per Liter" "pe / pH"
-axis_scale x_axis 0 1000 500
-axis_scale y_axis 1e-13 1500 auto auto log scale
-axis_scale sy_axis -14 21 3
-initial_solutions false
-plot_concentration_vs TOTAL_TIME
-start
10 GRAPH_X TOTAL_TIME/31556926
20 GRAPH_Y TOT("U")*238029, TOT("Se")*78960, TOT("As")*74922,
TOT("Mn")*54938, TOT("Fe")*55845, TOT("S(6)")*32065, TOT("Ra")*226000*1e9,
MOL("RaX2")
#Multipliers after each variable are to convert to mg/L from Molality,
then to pCi/L for Ra
30 GRAPH_SY LOG10(ACT("e-"))*-1, LOG10(ACT("H+"))*-1
-end
END
```

DATABASE C:\Program Files (x86)\USGS\Phreeqc Interactive  
2.18.5314\database\l1n1.dat

SOLUTION 0 source solution - from Monitoring well M-63

temp	13.86	#field measured
pH	7.4	#field measured
pe	2.63	#field measured
units	mg/l	
density	1	
Ca	61	
Cl	8 (charge)	0
F	0.1	
Mg	14	
Na	61	
K	6	
S(6)	10	
Fe	1.95	
Mn	0.06	
Se	0.0005	# 1/2 Det. Lim.
U	0.0967	
Ra	3.8e-9	# see notes for conversion (3.8pCi/L)
Ba	0.3	
As	0.0005	# 1/2 Det. Lim.
C(4)	359	
N(-3)	0.2	
N(5)	0.0	# 1/2 Det. Lim.
-water	1	# kg

SOLUTION 1-12 source solution - from Monitoring well M-63

temp	13.86	
pH	7.4	
pe	2.63	
redox	pe	
units	mg/l	
density	1	
Ca	61	
Cl	8 (charge)	0
F	0.1	
Mg	14	
Na	61	
K	6	
S(6)	10	
Fe	1.95	
Mn	0.06	
Se	0.0005	
U	0.0967	
Ra	3.8e-009	
Ba	0.3	
As	0.0005	
C(4)	359	
N(-3)	0.2	
N(5)	0	

-water 1 # kg  
SOLUTION 13-14 Downgradient Monitoring Well M-36

temp 12.45  
pH 7.83  
pe 1.76  
redox pe  
units mg/l  
density 1  
Ca 43  
Cl 3 (charge) 0  
F 0.2  
Mg 8  
Na 50  
K 6  
S(6) 100  
Fe 0.3  
Mn 0.03  
Se 0.0005  
U 0.0104  
Ra 4.5e-009  
Ba 0.02  
As 0.0005  
C(4) 178  
N(-3) 0.22

-water 1 # kg  
SOLUTION 15-20 Solution downgradient from Mine Area - MP-21

temp 13.6  
pH 6.94  
pe 0.114  
redox pe  
units mg/l  
density 1  
Ca 65  
Cl 17 (charge) 0  
F 0.05 #1/2 detection limit  
Mg 11  
Na 101  
K 7  
S(6) 122  
Fe 1.69  
Mn 0.28  
Se 0.008  
U 1.78  
Ra 7.95e-007  
Ba 0.3  
As 0.141  
C(4) 331  
N(-3) 0.33  
-water 1 # kg

SOLUTION 21-22 Downgradient Monitoring Well M-36

temp	12.45	
pH	7.83	
pe	1.76	
redox	pe	
units	mg/l	
density	1	
Ca	43	
Cl	3 (charge)	0
F	0.2	
Mg	8	
Na	50	
K	6	
S(6)	100	
Fe	0.3	
Mn	0.03	
Se	0.0005	
U	0.0104	
Ra	4.5e-009	
Ba	0.02	
As	0.0005	
C(4)	178	
N(-3)	0.22	
-water	1 # kg	

EQUILIBRIUM\_PHASES 1-12 #upgradient/oxidized

quartz	0	1
k-feldspar	0	.5
montmor-k	0	.2

EQUILIBRIUM\_PHASES 13-14 #downgradient/reduced w/ hfo

goethite	0	.01
quartz	0	1
k-feldspar	0	.5
Pyrite	0	1.2
montmor-k	0	.2
Uraninite	0	0
Coffinite	0	0
Calcite	0	0
Ferroselite	0	0
Siderite	0	0
gypsum	0	0
Se	0	0
RaSO4	0	0
Barite	0	0

EQUILIBRIUM\_PHASES 15-20 #transition zone/mine area

uraninite	0	.1
coffinite	0	.1
quartz	0	1
k-feldspar	0	.5
siderite	0	0
montmor-k	0	.2
orpiment	0	0
realgar	0	0

EQUILIBRIUM\_PHASES 21-22 #downgradient/reduced w/ hfo

goethite 0 .01  
quartz 0 1  
k-feldspar 0 .5  
Pyrite 0 1.2  
montmor-k 0 .2  
Uraninite 0 0  
Coffinite 0 0  
Calcite 0 0  
Ferroselite 0 0  
Siderite 0 0  
gypsum 0 0  
Se 0 0  
RaSO4 0 0  
Barite 0 0  
orpiment 0 0  
realgar 0 0

SOLUTION\_SPECIES

1.0000 H2AsO4- + 1.0000 F- = AsO3F-- +1.0000 H2O  
-llnl\_gamma 4.0  
log\_k -40

1.0000 H2AsO4- + 1.0000 H+ + 1.0000 F- = HAsO3F- +1.0000 H2O  
-llnl\_gamma 4.0  
log\_k -46

EXCHANGE\_SPECIES

Ra+2 + 2X- = RaX2

log\_k .91 #need to find real constants for Ra

-gamma 5 0

delta\_h 4.5

SURFACE\_SPECIES # (data source = Dzombak and Morel, 1990; Table 10.6);  
(Bassot, Mallet, and Stammose, 2001)

Hfo\_wOH + CO3-2 + H+ = Hfo\_wOCO2- + H2O  
log\_k = 12.78

Hfo\_wOH + CO3-2 + 2H+ = Hfo\_wOCO2H + H2O  
log\_k = 20.37

Hfo\_wOH + As(OH)3 = Hfo\_wH2AsO3 + H2O  
log\_k 5.41

Hfo\_wOH + AsO4-3 + 3H+ = Hfo\_wH2AsO4 + H2O  
log\_k 29.31

Hfo\_wOH + AsO4-3 + 2H+ = Hfo\_wHASO4- + H2O  
log\_k 23.51

Hfo\_wOH + AsO4-3 = Hfo\_wOHasO4-3  
log\_k 10.58

Hfo\_wOH + Ra+2 = Hfo\_wORa+ + H+  
log\_k -3.5

```

Hfo_wOH + Ra+2 + H2O = Hfo_wORaOH + 2H+
log_k    -12.95

Hfo_wOH + Ca+2 = Hfo_wOCa+ + H+
log_k    -5

Hfo_wOH + Ca+2 + H2O = Hfo_wOCaOH + 2H+
log_k    -14.5

END
EXCHANGE 1-12
  X      0.7
  -equilibrate with solution 1
  #-pitzer_exchange_gammas true
EXCHANGE 13-14
  X      0.7
  -equilibrate with solution 13
  #-pitzer_exchange_gammas true
EXCHANGE 15-20
  X      0.7
  -equilibrate with solution 15
  #-pitzer_exchange_gammas true
EXCHANGE 21-22
  X      0.7
  -equilibrate with solution 21
  #-pitzer_exchange_gammas true
END
SURFACE 13
  #-equilibrate with solution 13
  Hfo_wOH Goethite      equilibrium_phase 0.2      53300
  Hfo_sOH Goethite      equilibrium_phase 0.005    53300
SURFACE 21
  #-equilibrate with solution 21
  Hfo_wOH Goethite      equilibrium_phase 0.2      53300
  Hfo_sOH Goethite      equilibrium_phase 0.005    53300
END

SOLID_SOLUTIONS 13-14
Ba(x)Ra(1-x)SO4
-comp1  Barite    0.00
-comp2  RaSO4     0.00
END
SOLID_SOLUTIONS 20-22
Ba(x)Ra(1-x)SO4
-comp1  Barite    0.00
-comp2  RaSO4     0.00
END

TRANSPORT
  -cells      22
  -shifts     49 # total simulation time = shifts * time
step

```

```

    -time_step          650167822 # seconds
    -boundary_conditions constant flux
    -lengths            22*50 #length of each cell, in meters (N cells
* cell length)
    -dispersivities     22*12.2 # Xu and Eckstein, (1995), calculate
for each flowpath
    -thermal_diffusion  2    3e-010
    -punch_cells        22
    -punch_frequency    1
    -multi_d            false

```

#### SELECTED\_OUTPUT

```

    -distance           true
    -time               true
    -step              true
    -ph                true
    -pe                true
    -ionic_strength     true
    -totals             U Se As Mn Fe S(6) Ra    #(mol/kgw) total for an
element
    -molalities         HCO3-  UO2+2  Cl-  Na+  #(mol/kgw of specific
species)
                        Ca+2  HS-  Fe+2  SO4-2
                        O2
    -equilibrium_phases Calcite  Goethite  Pyrite  S

```

#### USER\_GRAPH

```

    -headings Years U Se As Mn Fe SO4 Ra(pCi/L) RaX2 pe pH
    -chart_title "GW Solute Concentrations at POE (M63 -> M36)"
    -axis_titles "(Years)" "Milligrams per Liter" "pe / pH"
    -axis_scale x_axis 0 1000 500
    -axis_scale y_axis 1e-13 1500 auto auto log scale
    -axis_scale sy_axis -14 21 3
    -initial_solutions false
    -plot_concentration_vs TOTAL_TIME
    -start
    10 GRAPH_X TOTAL_TIME/31556926
    20 GRAPH_Y TOT("U")*238029, TOT("Se")*78960, TOT("As")*74922,
TOT("Mn")*54938, TOT("Fe")*55845, TOT("S(6)")*32065, TOT("Ra")*226000*1e9,
MOL("RaX2"), #SURF("Ra","Hfo")
    #Multipliers after each variable are to convert to mg/L from Molality,
then to pCi/L for Ra
    30 GRAPH_SY LOG10(ACT("e-"))*-1, LOG10(ACT("H+"))*-1
    -end

```

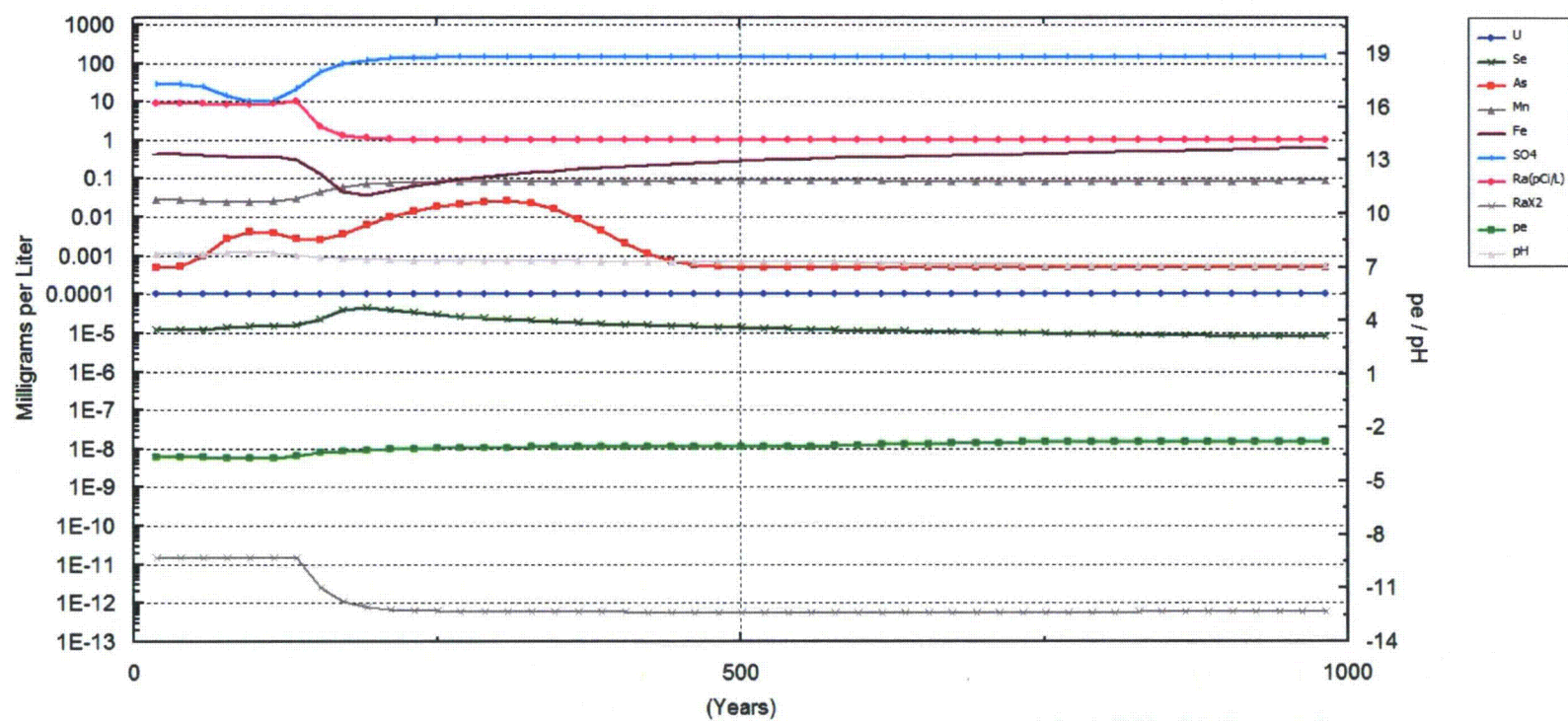
END



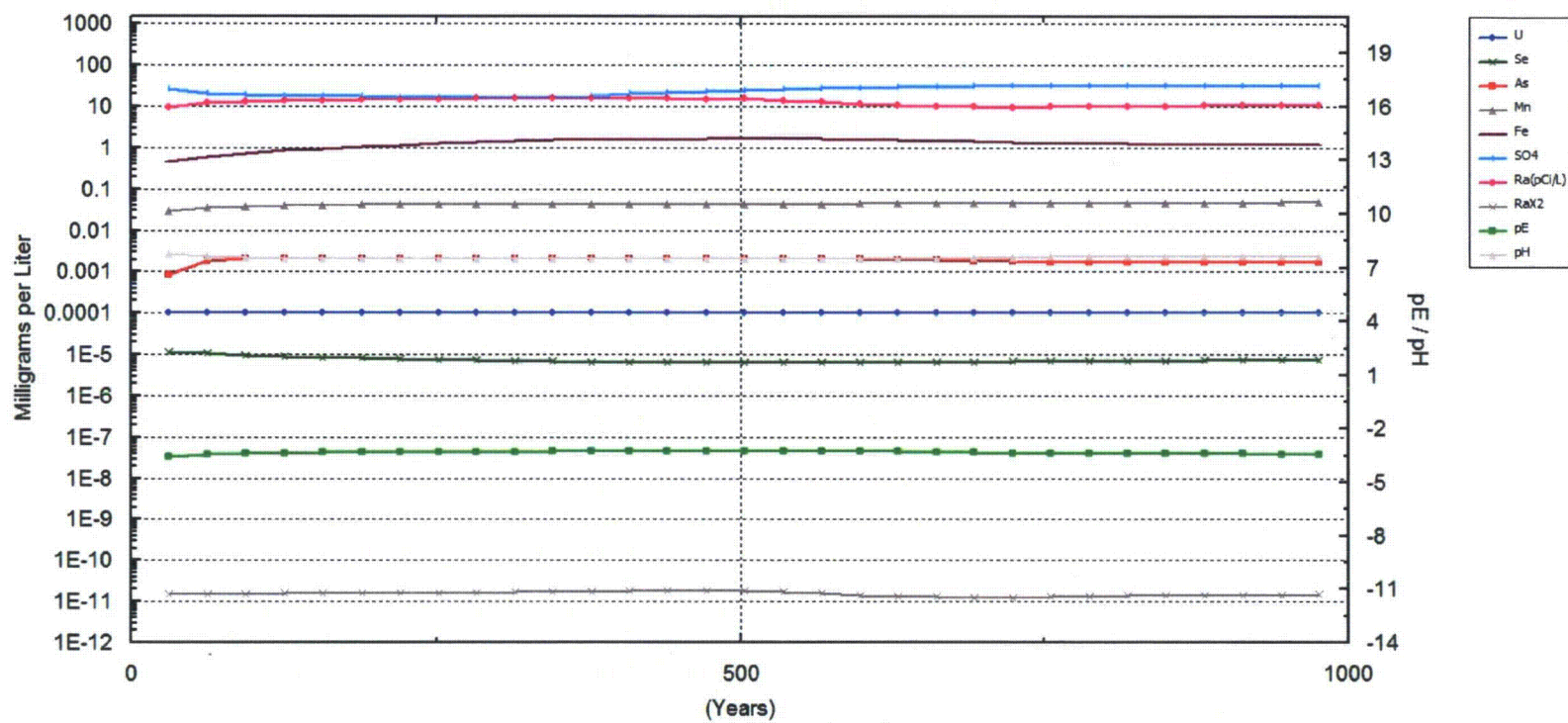
## **ATTACHMENT B**

**PHREEQC Graphical Output Constituent  
Concentration over Time at POE Wells for all Simulations**

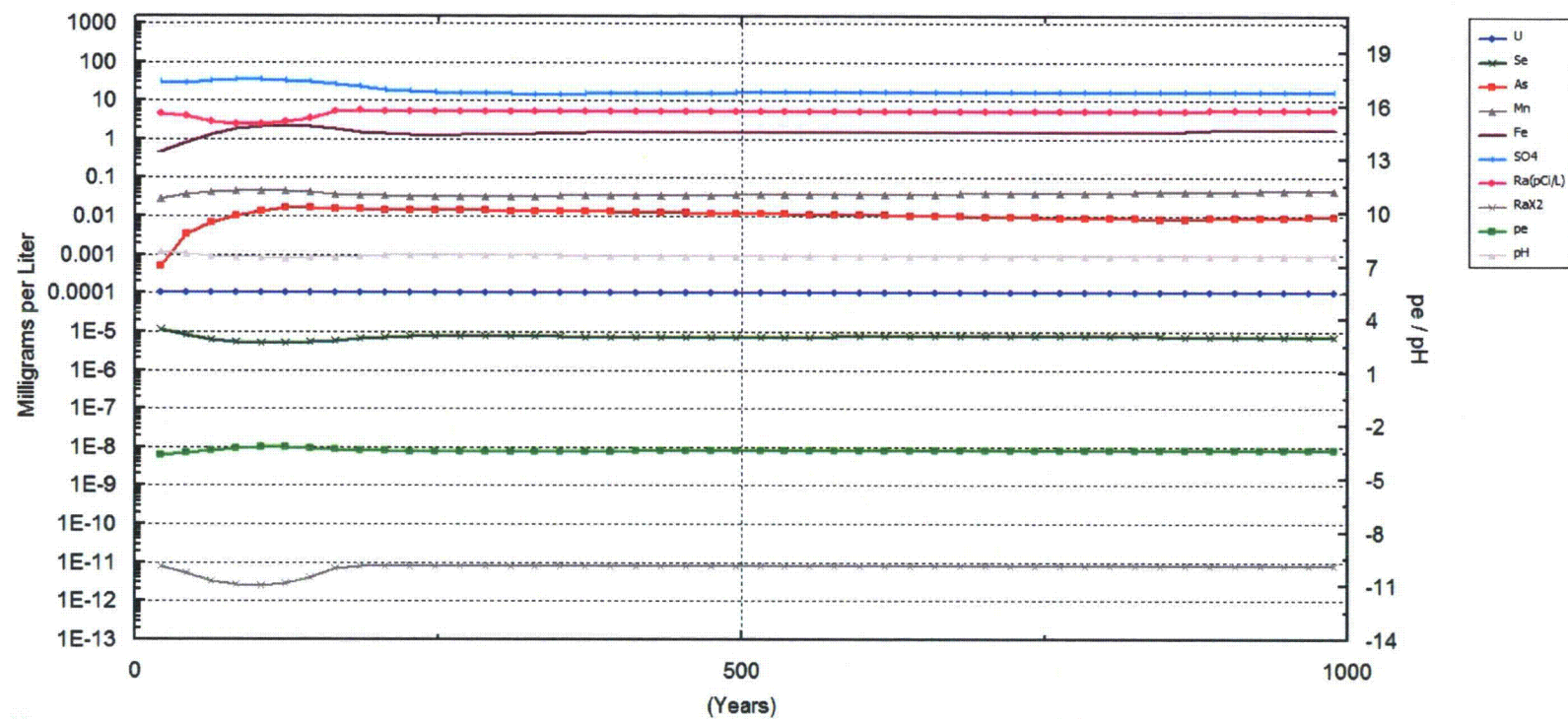
GW Solute Concentrations at POE (M56 -> M-24)



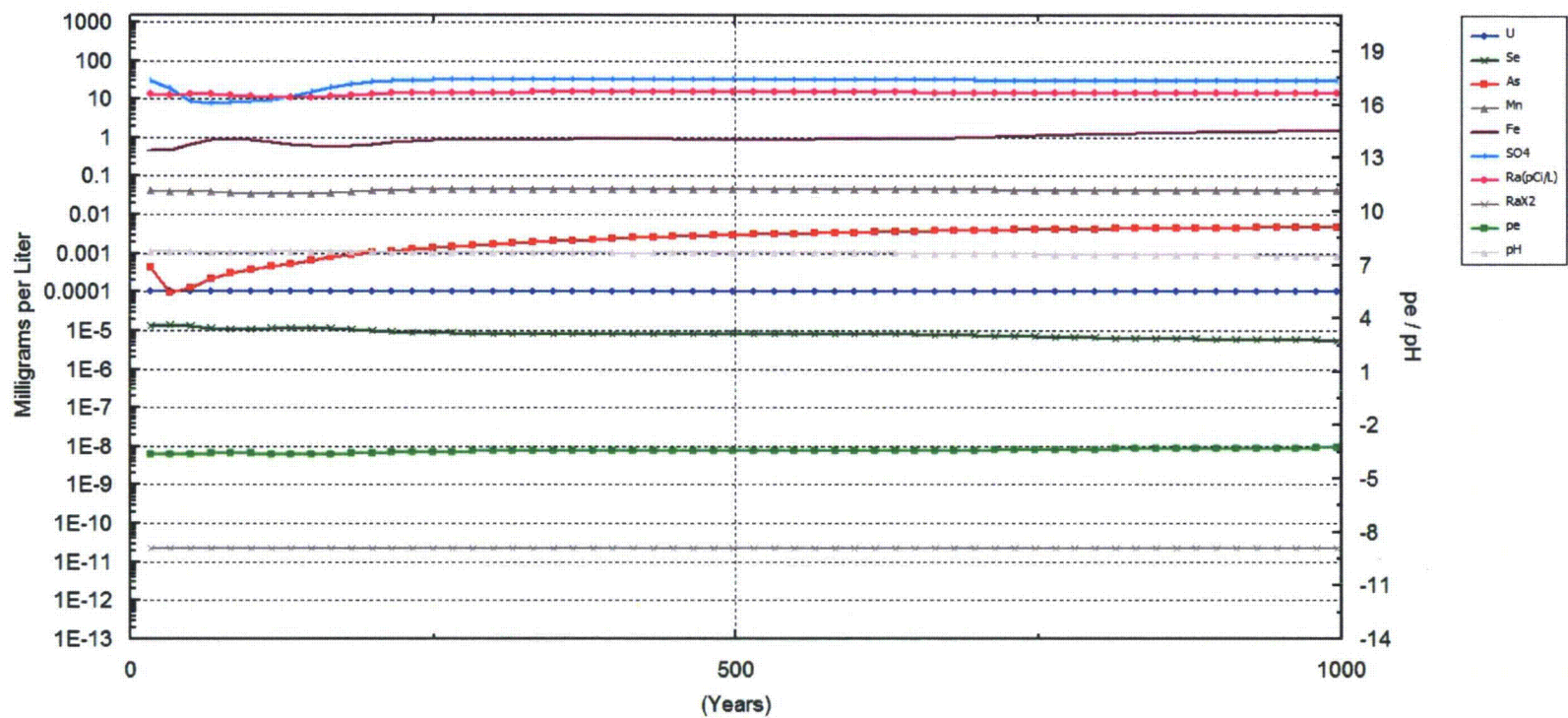
GW Solute Concentrations at POE (M55 -> M-24)



GW Solute Concentrations at POE (M63 -> M36)

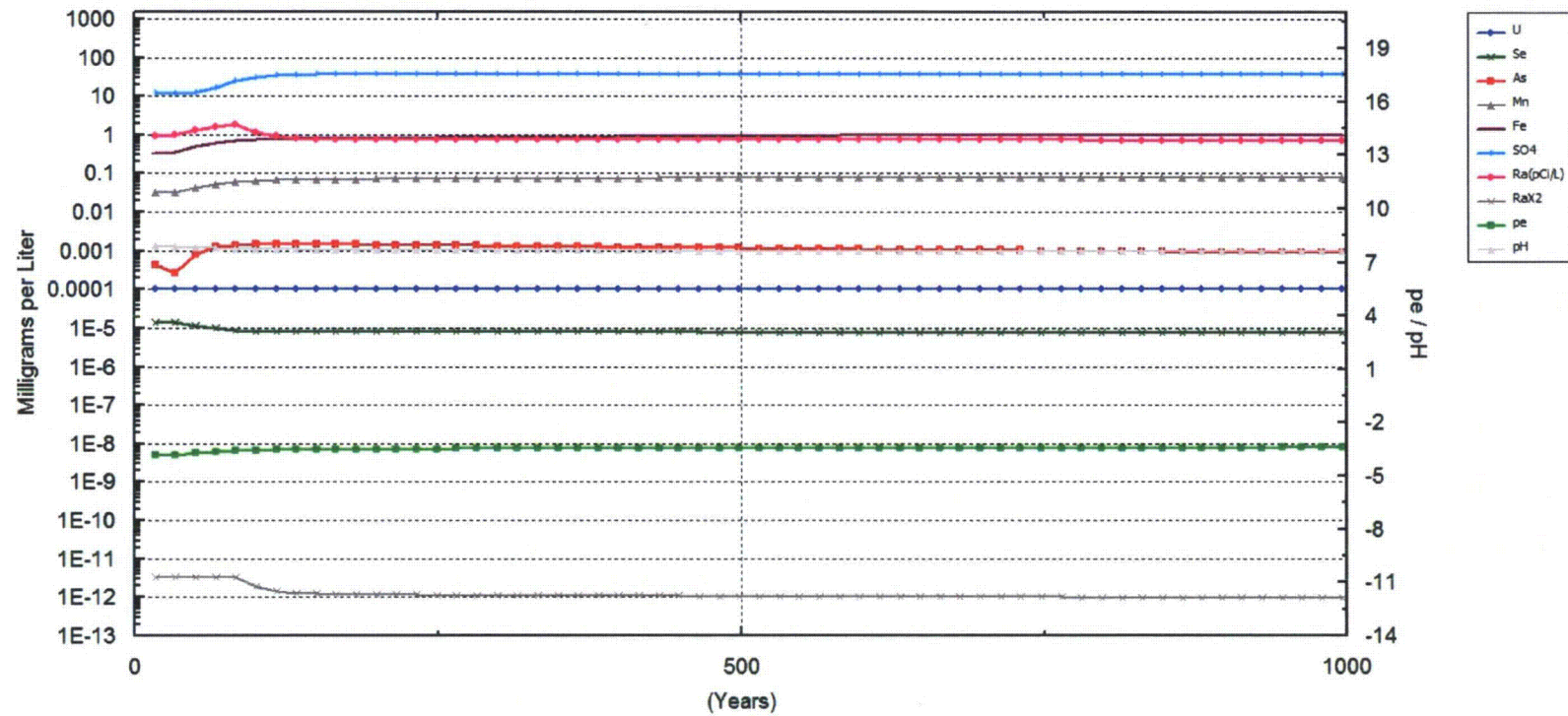


GW Solute Concentrations at POE (M-45 -> M-38)





GW Solute Concentrations at POE (M-44 -> M-37)



**APPENDIX B**  
**Hydrogeologic Assessment**

## **APPENDIX B**

### **Hydrogeologic Modeling of Groundwater in Mine Unit B of the Cameco Resources Highland Uranium Project Facility, Converse County, Wyoming**

***Prepared for:***

Cameco Resources (USA)  
2020 Carey Avenue, Suite 600  
Cheyenne, Wyoming, 82001

***Prepared by:***



INTERA Incorporated  
6000 Uptown Boulevard NE, Suite 220  
Albuquerque, New Mexico 87110

**March 09, 2012**





## EXECUTIVE SUMMARY

Groundwater in Mine Unit B has been affected by the dewatering and recovery of the ExxonMobil Highland open-pit and underground workings over the past 40 years. The AQUI-VER (2011) model is adopted in this study to determine the groundwater flow directions and velocities in the 30-Sand aquifer. The AQUI-VER (2011) model used the calibrated hydraulic parameters from the Lewis Water Consultants (2001) model, and it also extends the Lewis Water Consultants (2001) model to a larger area, including the Highland pit lake, and to more layers, including the 40-Sand and 50-Sand aquifers. The general pattern of groundwater flow in the 20-Sand and 30-Sand is similar, with groundwater flow toward the south and southeast across the Mine Unit B area, and the large majority of Mine Unit B groundwater flow ultimately captured by the Highland pit lake. A groundwater flow divide exists along the northern boundary of Mine Unit B in both the 30-Sand and 20-Sand aquifers, with the flow north of the divide ultimately discharging into the Box Creek drainage, and the flow south of the divide ultimately discharging into the Highland pit lake. MODPATH is used to calculate the groundwater velocities for the five particles, which are placed at the upgradient Point of Exposure wells in the 30-Sand aquifer within Mine Unit B. Results indicate that the average groundwater velocity ranges from 5.21 to 10.66 feet/year for the five particles along their pathlines.

## TABLE OF CONTENTS

<b>EXECUTIVE SUMMARY .....</b>	<b>1</b>
<b>LIST OF FIGURES .....</b>	<b>iii</b>
<b>LIST OF TABLES .....</b>	<b>iii</b>
<b>1.0 INTRODUCTION.....</b>	<b>1</b>
<b>2.0 CONCEPTUAL MODEL .....</b>	<b>2</b>
2.1 Geological Setting.....	2
2.2 Hydrogeological Setting .....	2
2.3 Alluvial Flow System Characteristics.....	3
<b>3.0 MODEL DESIGN .....</b>	<b>3</b>
3.1 Model Area and Grid .....	3
3.2 Boundary Conditions .....	3
3.3 Parameter Assignments.....	4
3.4 Water Budget .....	4
<b>4.0 MODEL CALIBRATION.....</b>	<b>5</b>
<b>5.0 MODEL RESULTS .....</b>	<b>6</b>
5.1 Distribution of Hydraulic Heads .....	6
5.2 Flow Pathlines.....	6
5.3 Groundwater Velocity.....	6
<b>6.0 REFERENCES.....</b>	<b>7</b>

## LIST OF FIGURES

Figure 1	Location Map
Figure 2	Modified Cross Section from Hunter, 1999
Figure 3	Model Domain and Grids
Figure 4	Model Boundary Conditions
Figure 5	Hydraulic Heads in the 30-Sand
Figure 6	Hydraulic Heads in the 20-Sand
Figure 7	Particle pathlines in the 30-Sand
Figure 8	Groundwater Velocities in the 30-Sand

## LIST OF TABLES

Table 1	Water budget from the steady-state groundwater flow model.....	5
Table 2	The groundwater velocities of the five particles along their pathlines in the 30-Sand. ....	7



---

## ACRONYMS AND ABBREVIATIONS

ft/day	feet per day
ft/yr	feet per year
ft <sup>3</sup> /day	cubic feet per day
HSU	Highland sandstone unit
POC	Point of Compliance
POE	Point of Exposure

## 1.0 INTRODUCTION

Groundwater in Mine Unit B of the Cameco Resources Highland Uranium Project facility has been affected by the dewatering and recovery of the ExxonMobil Highland open-pit and underground workings over the past 40 years. Different modeling efforts have been performed to investigate the groundwater flow conditions and fate transport within the aquifers (e.g., the 20-Sand, the 30-Sand, or the 40-Sand) in the area (Lewis Water Consultants, 2001; Aqui-Ver, 2011).

Lewis Water Consultants (2001) constructed a groundwater flow MODFLOW (McDonald and Harbaugh, 1988) model to identify the groundwater flow directions and velocities in the A- and B-Wellfield areas. The model only included two layers, which represented the 20-Sand and 30-Sand. They also constructed a geochemical model to simulate the fate and transport of chemical constituents in groundwater and to assess the impacts of the B-Wellfield restoration on the A-Wellfield water quality. The model results suggested that groundwater flows from the 20-Sand to the 30-Sand at a low rate during the B-Wellfield restoration, thereby precluding any significant impact on A-Wellfield water quality.

Aqui-Ver (2011) developed a three-dimensional groundwater flow model to simulate the future steady-state groundwater flow conditions based on the previously calibrated pre-In-Situ Recovery (ISR) model. This model was extended from the Lewis Water Consultants (2001) model and included two more overlying 40-Sand and 50-Sand aquifers. It was also expanded to include a larger area to the east of Mine Unit B and the Highland pit lake. Results indicated that the general pattern of groundwater flow in the 20-Sand, 30-Sand, and 40-Sand is very similar, with groundwater flow toward the south and southeast across the Mine Unit B area.

In order to determine the fate and transport of constituents in the Mine Unit B production zones (Point of Compliance [POC]) as groundwater migrates downgradient to the monitoring well ring (hereafter referred to as the Point of Exposure [POE] well ring), INTERA Inc. adopted the Aqui-Ver (2011) model to determine the directions and velocities of groundwater flow in the aquifers. Several particles are assigned at the upgradient POE Wells, and the track paths generated by MODPATH (Pollack, 1989) can simulate the path of a particle of water as it moves from upgradient, through the ISR production zone (POC wells), past the outer POE well, and ultimately to its discharge location.

## 2.0 CONCEPTUAL MODEL

### 2.1 Geological Setting

The Highland Uranium Project facility is located in the Powder River Basin, a structural and topographic basin that covers approximately 12,000 miles in the northeastern part of the state of Wyoming (Figure 1). Previous studies (Langen and Kidwell, 1974; Dahl and Hagmaier, 1976) identified a group of three distinctive fluvial channel sandstones that contain most of the uranium in the Highland Project area. The fluvial sandstone was named the Highland sandstone unit (HSU). The HSU is 120 to 150 feet thick, and is stratigraphically located in the Fort Union Formation (Figure 2). The HSU crops out east of the Highland Project area and dips gradually basinward and westward to a depth of around 1,000 feet near the project area. At the Highland Project area, the fluvial sand members of the HSU are identified as the 20-Sand, 30-Sand, 40-Sand, and 50-Sand, although other sand units are present in the area ranging from 10-Sand to 100-Sand (Figure 2). The sands are generally separated by silty claystone floodplain deposits, but may be in hydraulic communication in local areas if floodplain deposits are not present (Hunter, 1999). In this study, both the 30-Sand and 20-Sand are investigated. The 30-Sand near the Highland Project area is of main interest because it is the main production zone for Highland Project Mine Unit-B.

### 2.2 Hydrogeological Setting

The topography in the permit area is characterized by gently rolling upland areas and broad stream valleys that are dissected by numerous draws with relatively steep slopes and rounded ridge crests. The primary surface drainages include the Box Creek, Duck Creek, Willow Creek, and Brown Springs Creek of the Cheyenne River drainage system. All streams are ephemeral and flow only in response to snow melt and heavy thunderstorms that account for approximately 12 inches of precipitation annually.

The hydrogeologic units beneath the permit area and in the general vicinity include the following: Holocene-age alluvial deposits, the Eocene-age Wasatch Formation, the Paleocene-age Fort Union Formation, and the Cretaceous-age Lance and Fox Hills Formations. Individual sandstones within these units may be classified as aquifers depending on their hydrologic characteristics and potential yield to wells and/or springs.

Aquifer of interest to the study is mainly the 30-Sand (Mine Unit B production zone). In addition, the model in the study includes the 20-Sand (underlying aquifer), 40-Sand and 50-Sand (overlying aquifers). These aquifers are part of a sequence of permeable sands separated by lower permeability claystone, siltstone and shale aquitards of the lower Wasatch Formation of

fluvial origin (Aqui-Ver, 2011). Furthermore, the aquitard separating the 20-Sand and 30-Sand is thin or missing in the northern and central portion of Mine Unit B due to erosion by the overlying 30-Sand, thereby yielding an area of hydraulic connection. On the other hand, the aquitard separating the 30-Sand and the overlying 40-Sand is more uniform and consistent, which acts as a barrier for vertical groundwater flow across the mine unit (Aqui-Ver, 2011).

### **2.3 Alluvial Flow System Characteristics**

Estimates of hydraulic conductivity for the 20-Sand and 30-Sand are obtained from the results of aquifer test data collected prior to the start-up of ISR in the A- and B-Wellfields (Lewis Water Consultants, 2001). Hydraulic conductivities of both the 20-Sand and 30-Sand are relatively uniform, with a range of 0.6 to 2.8 feet per day (ft/day) for the 20-Sand, and 1.6 to 2.7 ft/day for the 30-Sand (Lewis Water Consultants, 2001). The vertical hydraulic conductivity of the in-between aquitard was assigned an initial value of  $3 \times 10^{-5}$  ft/day in their model based on results of aquifer test leakance calculations (1987 20-Sand pump test) and laboratory testing of aquitard materials (Lewis Water Consultants, 2001). The groundwater model (Lewis Water Consultants, 2001) developed for the A- and B-Wellfields was calibrated with a hydraulic conductivity of 2.2 ft/day for the 30-Sand and 0.7 ft/day for the 20-Sand, and a vertical hydraulic conductivity of  $2 \times 10^{-4}$  ft/day for the in-between aquitard in the Mine Unit B area. Based on the lithology of the alluvium, porosity is estimated to range from 0.15 to 0.25 (Fetter, 1989). In this study, a value of 0.2 is used to represent the porosity.

## **3.0 MODEL DESIGN**

### **3.1 Model Area and Grid**

The Aqui-Ver (2011) steady-state MODFLOW groundwater flow model is used in this study. Figure 3 shows the model domain and grids. This model includes six layers; however, layers 1 and 2 are considered as inactive layers with the other four layers representing the 50-Sand, 40-Sand, 30-Sand, and 20-Sand in Mine Unit B, respectively. In each layer, the model is discretized into 100 rows and 139 columns (Figure 3). There are a total of 83,400 cells; 54,279 of them are active. A uniform grid spacing of 200 ft is applied to the whole model area.

### **3.2 Boundary Conditions**

According to the Aqui-Ver (2011) model, the boundary conditions were modified from the Lewis Water Consultants (2001) model to include a larger area to the east of Mine Unit B and the Highland pit lake. The Aqui-Ver (2011) model uses Constant Head Boundaries in the aquifers to represent the discharge locations (outcrops) or the regional formation dip (Figure 4).

General Head Boundaries are used at model edges to incorporate the estimated pre-uranium recovery regional groundwater flow direction (southeast/east) toward discharge locations in the drainage of the Box Creek (Figure 4). General Head Boundary conductance was assigned based on the hydraulic conductivity of aquifer materials and the estimated elevation and distance to known recharge and discharge areas. In addition, groundwater recharge was applied to the top active layer (50-Sand). The recharge rate was assigned a value of 0.0044 inches/year. Also, an evaporation rate of 16.2 inches/year was assigned at the Highland pit lake.

### **3.3 Parameter Assignments**

Four aquifers are simulated in the model to represent the 50-Sand, 40-Sand, 30-Sand, and 20-Sand, respectively, where 30-Sand is the Mine Unit B production zone. The order of the four aquifers from top to bottom is 50-Sand, 40-Sand, 30-Sand, and 20-Sand. Lewis Water Consultants (2001) calibrated the hydraulic conductivities for the 20-Sand and 30-Sand, which resulted in a hydraulic conductivity of 0.7 ft/day for the 20-Sand and 2.2 ft/day for the 30-Sand in the A- and B-Wellfield areas. The vertical hydraulic conductivity for the aquitard between the 20-Sand and 30-Sand is  $2 \times 10^{-4}$  ft/day. For the 40-Sand and 50-Sand, a hydraulic conductivity of 1.5 ft/day is used for the Mine Unit B in the AQUI-Ver (2011) model. These aquifers may be separated by low-permeability claystone, siltstone, and shale aquitards of the lower Wasatch Formation, which is of fluvial origin (Hunter, 1999; AQUI-Ver, 2011). However, the aquitard might be thin or missing in areas due to the erosion of the aquifers, which can result in areas of hydraulic connection. In the AQUI-Ver (2011) model, the specific storage is  $7.5 \times 10^{-5}$  1/ft for 50-Sand, 40-Sand, and 30-Sand, and  $2.0 \times 10^{-4}$  1/ft for 20-Sand. Moreover, an effective porosity of 0.2 is used to compute groundwater flow velocity.

### **3.4 Water Budget**

The water balance fluxes are calculated for the steady-state groundwater flow model (Table 1). The total mass balance error was -0.0002%. Inflows to the model include groundwater recharge and flow from the Constant Head and General Head Boundaries. General Head Boundaries are used to simulate regional groundwater flow direction and are incorporated at the model edges; thus, they account for most of the total mass balance (81.2%). Outflows of the model include evaporation and flow out of the Constant Head and General Head Boundaries, with both boundaries being simulated as discharge locations. Evaporation is the main outflow for the total mass balance of the whole model (56.7%).



**Table 1. Water Budget from the Steady-State Groundwater Flow Model**

<b>Water Balance Component</b>	<b>Flux Rate (ft<sup>3</sup>/day)</b>	<b>Percent Total</b>
<b>Inflow</b>		
Groundwater Recharge	540.3	1.8
Leakage from Constant Head BC	5,005.7	17.0
Influx from General Head BC	23,959.8	81.2
<i>Total In:</i>	<i>29,505.8</i>	
<b>Outflow</b>		
Evaporation	16,724.0	56.7
Discharge from Constant Head BC	4,402.1	14.9
Outflux from General Head BC	8,379.7	28.4
<i>Total Out:</i>	<i>29,505.8</i>	
<b>Mass Balance Error (percent error)</b>	<b>-0.0002</b>	

## 4.0 MODEL CALIBRATION

Model calibration is the process of making changes to the hydraulic properties and other inputs in the groundwater flow model so that the simulated groundwater levels match observed groundwater levels closely. In this study, the AQUI-VER (2011) model is adopted. This model has more layers and a larger area than the Lewis Water Consultants (2001) model. Lewis Water Consultants (2001) calibrated their steady-state model using the water level data collected in January of 2000 (20-Sand) and December of 2000 (30-Sand). After calibration, they obtained the hydraulic conductivity of 0.7 ft/day for the 20-Sand and 2.2 ft/day for the 30-Sand, which are used in the AQUI-VER (2011) model. Furthermore, because the AQUI-VER (2011) model expanded the original Lewis Water Consultants (2001) model, this model was re-calibrated to estimated pre-uranium recovery water level elevations. The AQUI-VER (2011) groundwater flow model was modified to simulate pre-uranium recovery conditions by removing the Highland pit and Exxon underground workings from the model (simulated by replacing the void space with native aquifer material) and removing the constant head boundary condition representing evaporation from the pit lake. Then the model was run forward to a steady-state condition representative of a pre-ISR condition. After that, the model was run forward to simulate the steady-state filling of the Highland pit lake and recovery of the aquifer system. Steady-state pit lake inflows, outflows, and water levels were compared to results presented by ExxonMobil (2007). The AQUI-VER (2011) model suggested a reasonable representation of pre-ISR conditions based on the steady-state flow calibration.

## **5.0 MODEL RESULTS**

### **5.1 Distribution of Hydraulic Heads**

Figures 5 and 6 show the hydraulic heads and groundwater flow directions in the 30-Sand and 20-Sand aquifers based on the steady-state groundwater flow model. The interval of the contours is 2 ft. For the whole model area, groundwater flow generally flows from west to east, and two apparent discharge locations are the Highland pit lake and the Box Creek. The elevation of the Highland pit lake is about 5,060 ft.

In terms of the Mine Unit B area, the aquitard separating the 20-Sand and 30-Sand is thin or missing in the northern and central portion of Mine Unit B, thereby resulting in areas of hydraulic connection between the two aquifers. Results suggest that the general pattern of groundwater flow in the 20-Sand and 30-Sand is predicted to be similar, with groundwater flow toward the south and southeast across the Mine Unit B area, with the large majority of Mine Unit B groundwater flow ultimately captured by the Highland pit lake.

A groundwater flow divide is predicted to exist along the northern boundary of Mine Unit B in both the 30-Sand and 20-Sand aquifers, with the flow north of the divide ultimately discharging into the Box Creek drainage, and the flow south of the divide ultimately discharging into the Highland pit lake.

### **5.2 Flow Pathlines**

Five particles are assigned in layer 5 (30-Sand), and their locations are at upgradient POE wells M-56, M-55, M-63, M-45, and M-44. MODPATH (Pollack, 1989) is used to identify the flow pathlines for the five particles (Figure 7). Of the five particles, only one particle located in the northern portion of Mine Unit B has a flow path toward the Box Creek, whereas the other four particles all have flow paths toward the Highland pit lake. It is suggested that there is a divide in the northern portion of Mine Unit B at which groundwater discharges to different locations. Since the distance between Mine Unit B and the Highland pit lake is much shorter than the distance between Mine Unit B and the Box Creek, it would take much longer for the particles located in the northern portion of Mine Unit B to discharge to the Box Creek.

### **5.3 Groundwater Velocity**

MODPATH can calculate the groundwater flow velocity in the 30-Sand aquifer (Figure 8). Groundwater velocity ranges from 1.57 to 50.69 ft/year for the five particles along their pathlines. Furthermore, the groundwater velocity is much higher near the discharge locations, e.g., the Box Creek and the Highland pit lake, due to the higher hydraulic gradients of the

discharge areas. The average groundwater velocities for the five particles along their pathlines range from 5.21 to 10.66 ft/year, as shown in Table 2. Data from these track paths are used to create a geochemical transport model in PHREEQC (Parkhurst and Appelo, 1999).

**Table 2. The Groundwater Velocities of the Five Particles along Their Pathlines in the 30-Sand**

Upgradient POE Well	POC Well	Downgradient POE Well	Maximum Groundwater Velocity (ft/year)	Minimum Groundwater Velocity (ft/year)	Average Groundwater Velocity (ft/year)
M-56	MP-12	M-24	50.69	1.84	8.52
M-55	MP-16	M-24	12.38	1.57	5.21
M-63	MP-21	M-36	19.06	3.82	7.96
M-45	MP-27	M-38	19.13	5.19	10.66
M-44	MP-26	M-37	17.44	5.28	9.88

## 6.0 REFERENCES

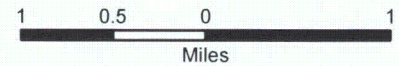
- Aqui-Ver Inc. 2011. Mine Unit B Hydrologic Assessment, Cameco Resources Highland Uranium Project, Converse County, Wyoming.
- Dahl, A.R. and Hagmaier, J.L. 1976. Genesis and Characteristics of the Southern Powder River Basin Uranium Deposits, Wyoming. Wyoming Geological Association, 28th Annual Field Conference Guidebook, p.243-252.
- ExxonMobil. 2007. Long Term Geochemical Evolution of the Highland Pit Lake.
- Fetter, C.W. 1989. Applied Hydrogeology. Macmillan: New York, New York, 592 pp.
- Hunter, J. 1999. Fluvial Architecture and Paleo-Ground Water Infiltration of the Fort Union Formation near the Highland Uranium Mine, Southern Powder River Basin, Wyoming. Coalbed Methane and the Tertiary Geology of the Powder River Basin, Wyoming and Montana, 50<sup>th</sup> Annual Field Conference Guidebook.
- Langen, R.E. and Kidwell, A.L. 1974. "Geology and Geochemistry of the Highland Uranium Deposit, Converse County, Wyoming." The Mountain Geologist, Vol.11, No.2, P.85-93.
- Lewis Water Consultants, Inc. 2001. Geochemical Transport Modeling of Wellfield Restoration by Natural Attenuation.
- McDonald, M.G. and Harbaugh, A.W. 1988. A Modular Three-Dimensional Finite-Difference Ground-Water Flow Model, Techniques of Water-Resources Investigations of the United States Geological Survey, Book 6, Chapter A1, Modeling Techniques.



- 
- Parkhurst, D.L. and Appelo, C.A.J. 1999. User's Guide to PHREEQC (Version 2) – A Computer Program for Speciation, Batch-Reaction, One-Dimensional Transport, and Inverse Geochemical Calculations. U.S. Geological Survey Water-Resources Investigation Report 99-4259.
- Pollack, D.W. 1989. Documentation of Computer Programs to Compute and Display Pathlines Using Results from the U.S. Geological Survey Modular Finite Difference Flow Model, U.S. Geological Survey Open-File Report 89-381.

## Figures



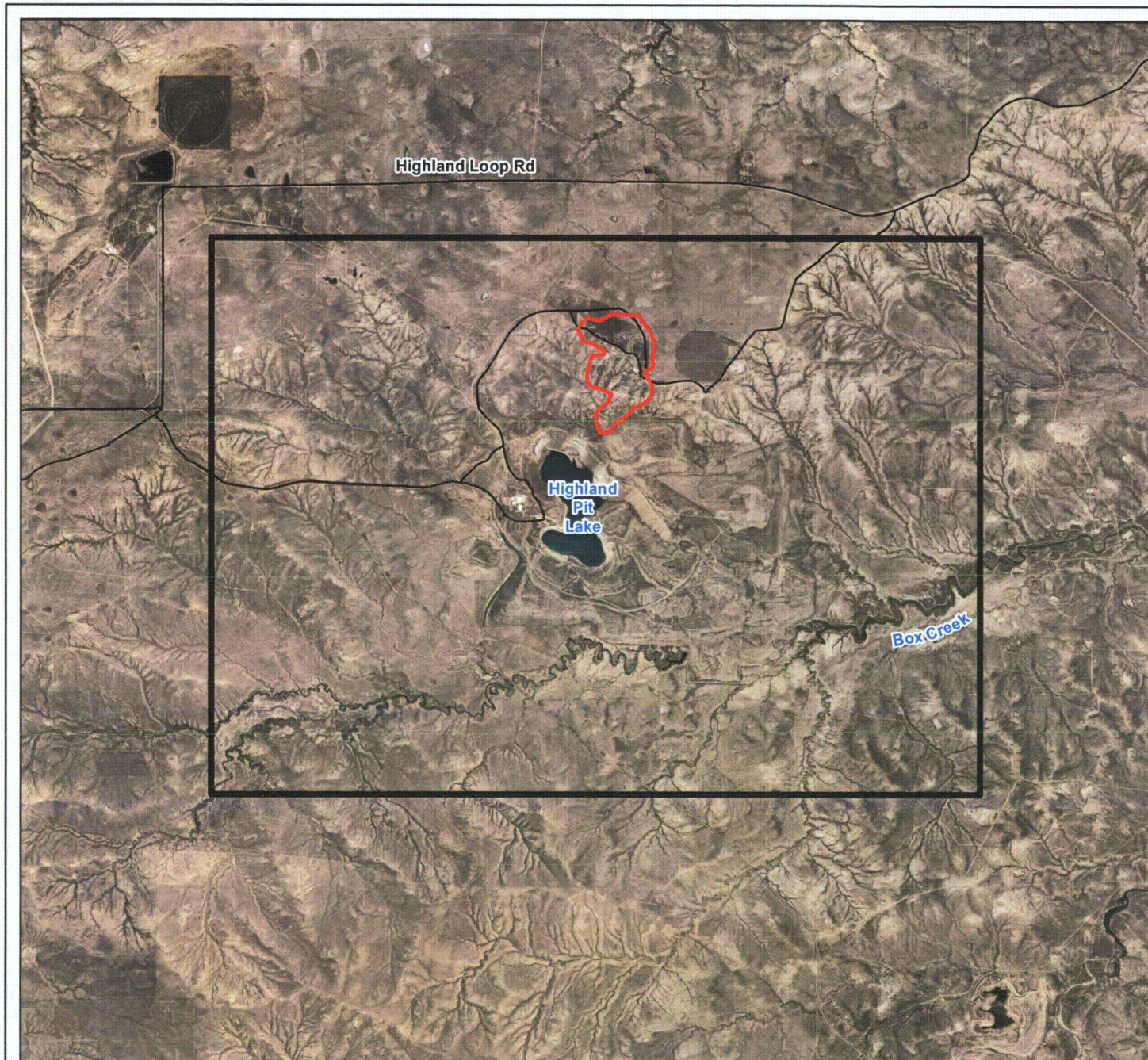


### Legend

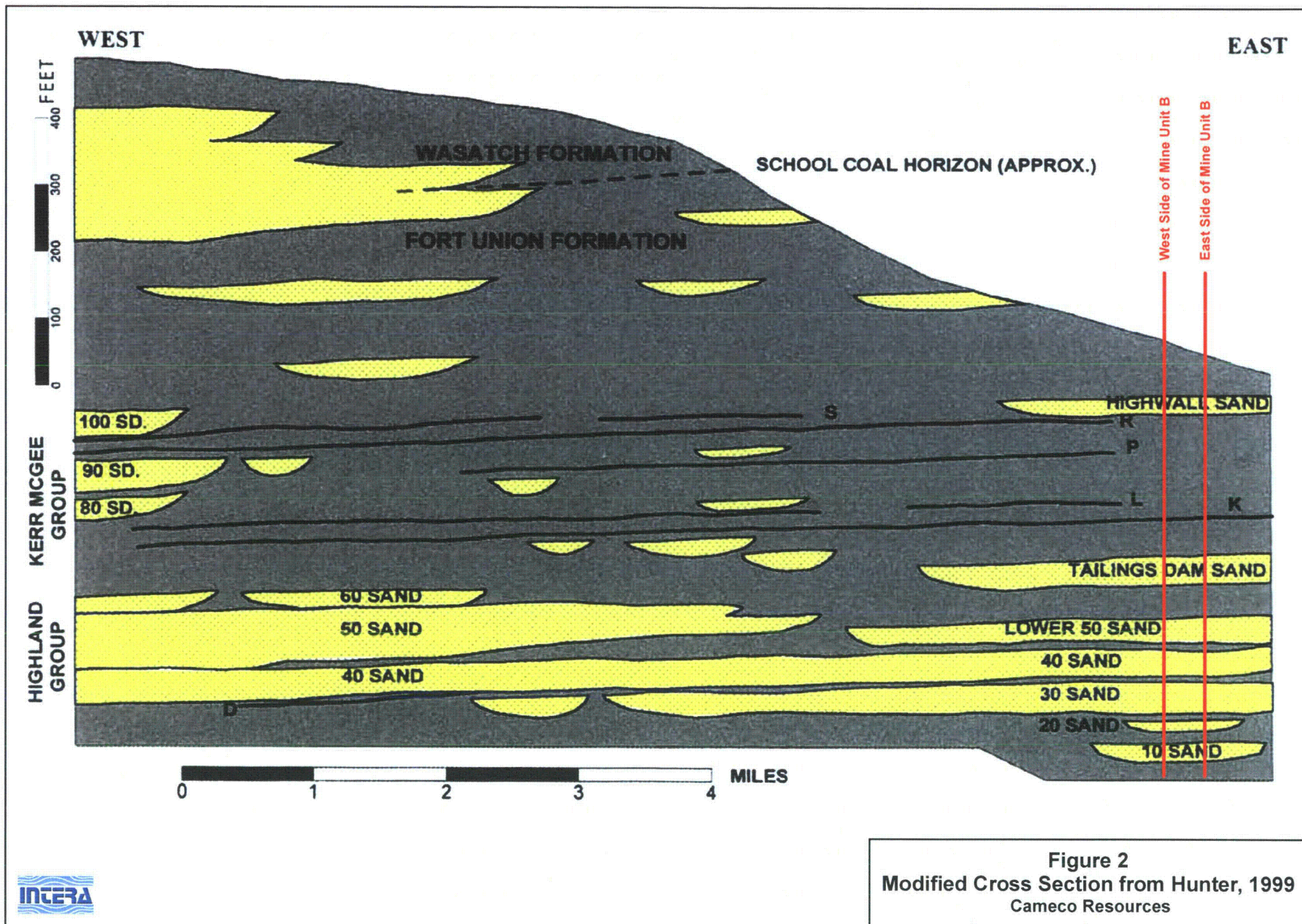
- Mine Unit-B
- Model Domain



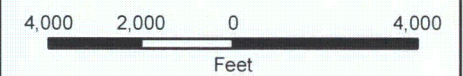
**Figure 1**  
**Location Map**  
**Cameco Resources**





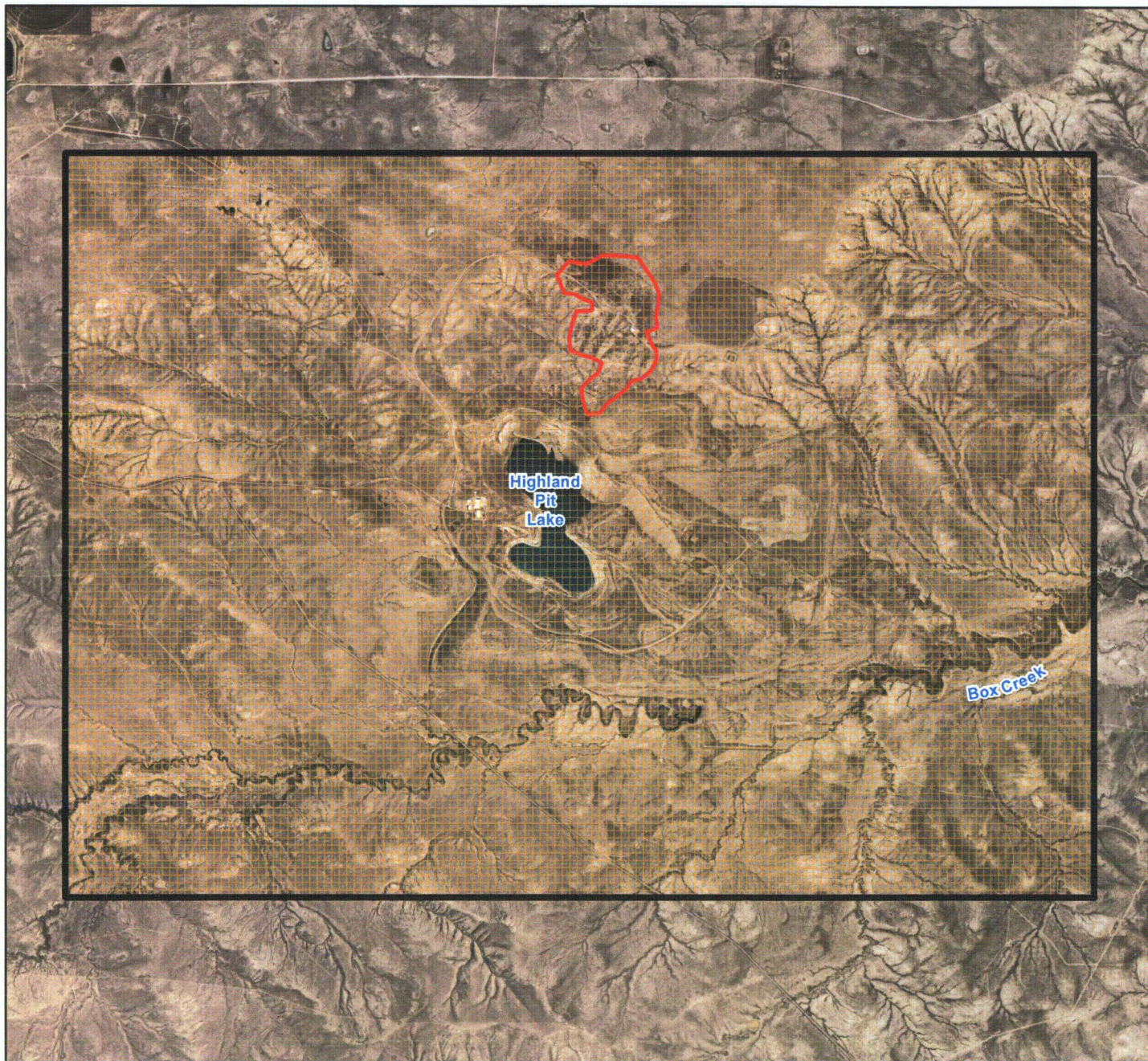






### Legend

-  Mine Unit-B
-  Model Grid
-  Model Domain






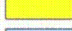
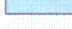
**Figure 3**  
**Model Domain and Grids**  
Cameco Resources





4,000 2,000 0 4,000  
Feet

#### Legend

-  Mine Unit-B
-  Model Grid
-  Model Domain
-  Constant Head BC
-  GHB BC

**Figure 4**  
**Model Boundary Conditions**  
**Cameco Resources**



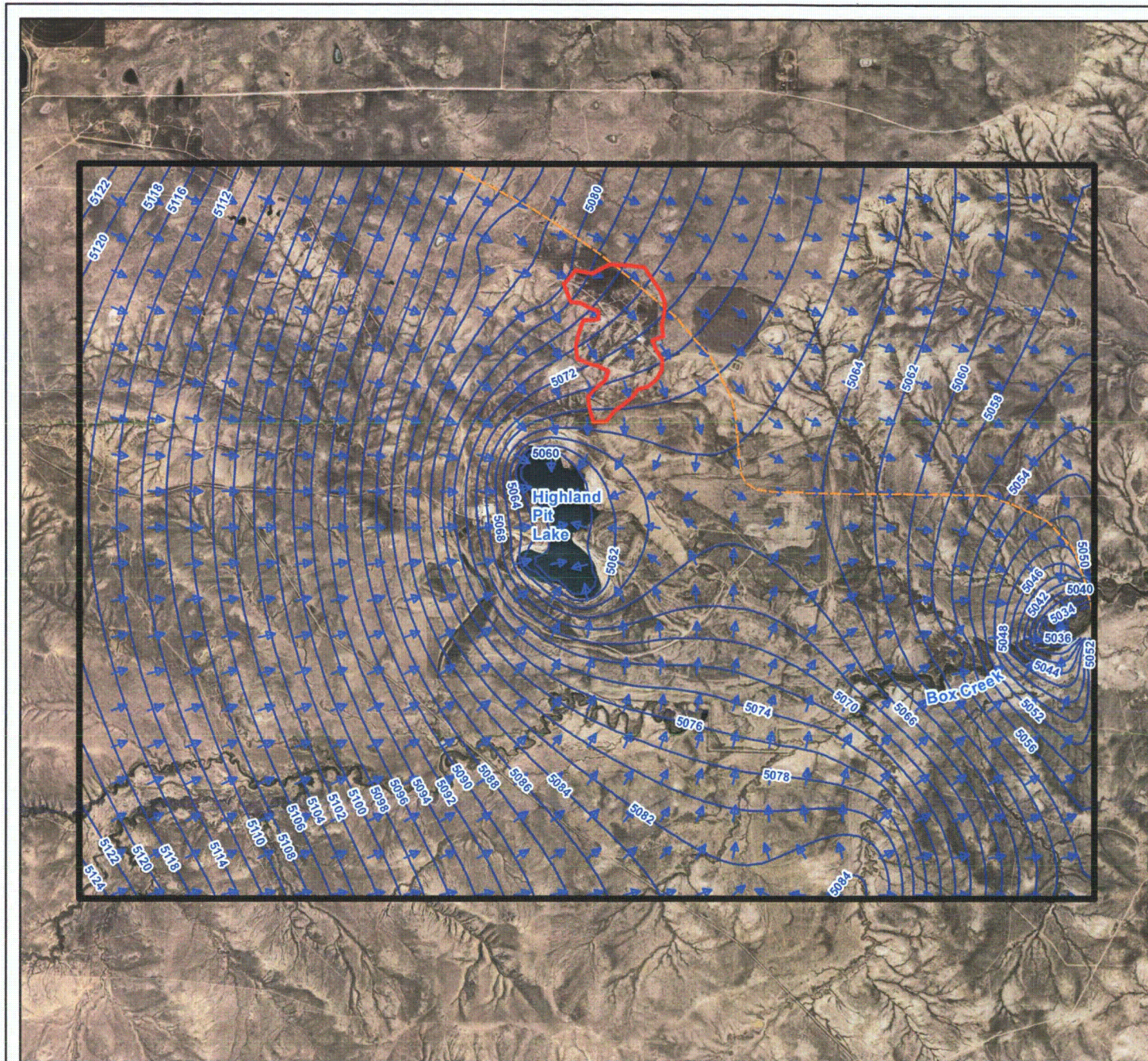


4,000 2,000 0 4,000  
Feet

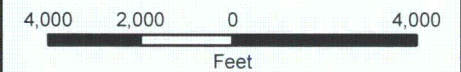
### Legend

- Groundwater Elevation (ft-amsl)
- Groundwater Flow Direction
- - - Groundwater Flow Divide
- ▭ Mine Unit-B
- ▭ Model Domain

**Figure 5**  
**Hydraulic Head**  
**in the 30-Sand**  
**Cameco Resources**



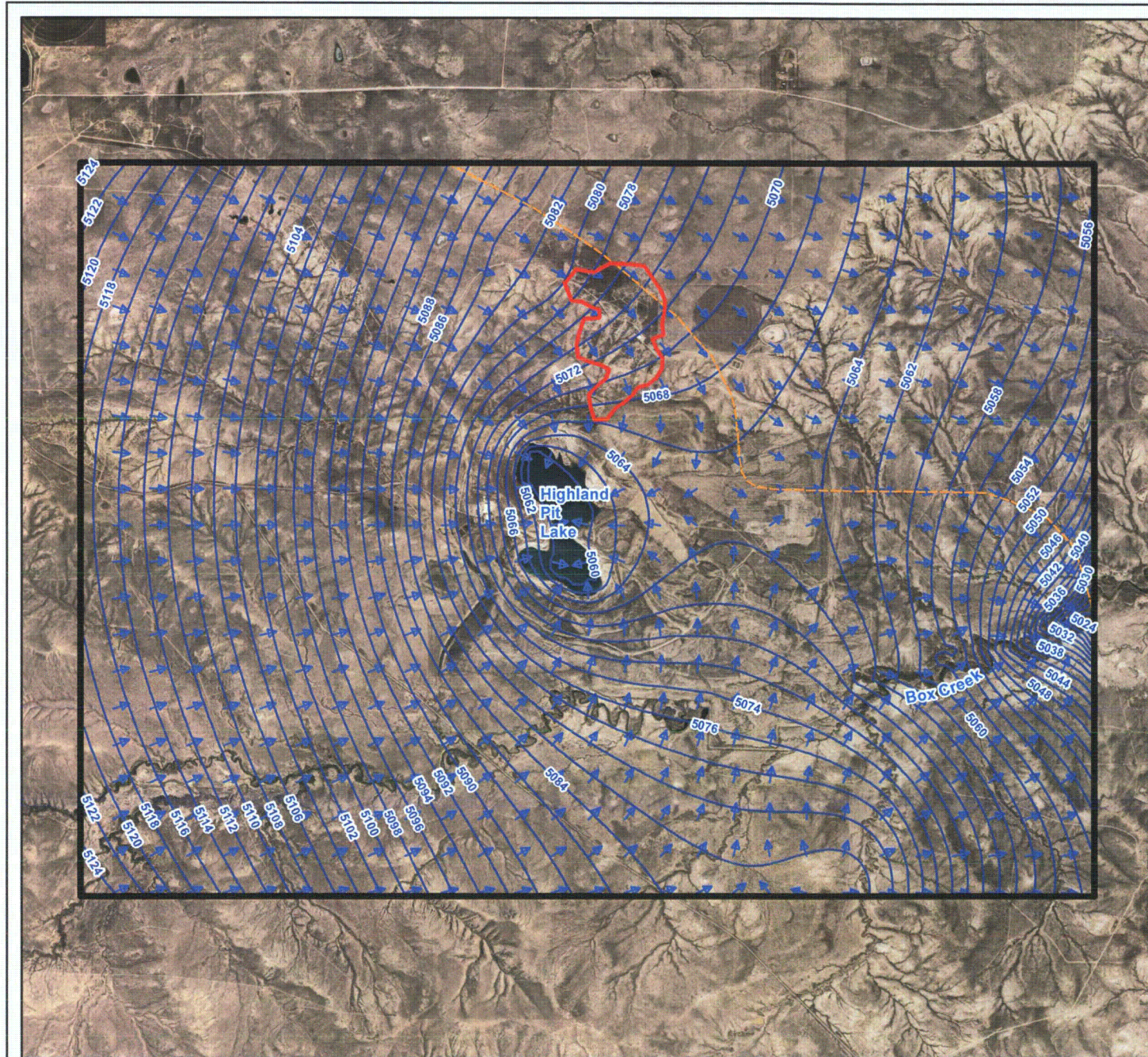




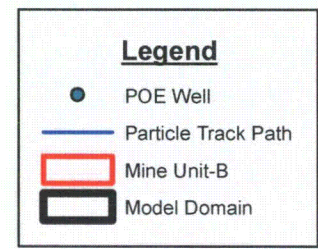
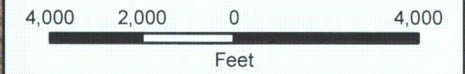
### Legend

- Groundwater Elevation (ft-amsl)
- Groundwater Flow Direction
- Groundwater Flow Divide
- Mine Unit-B
- Model Domain

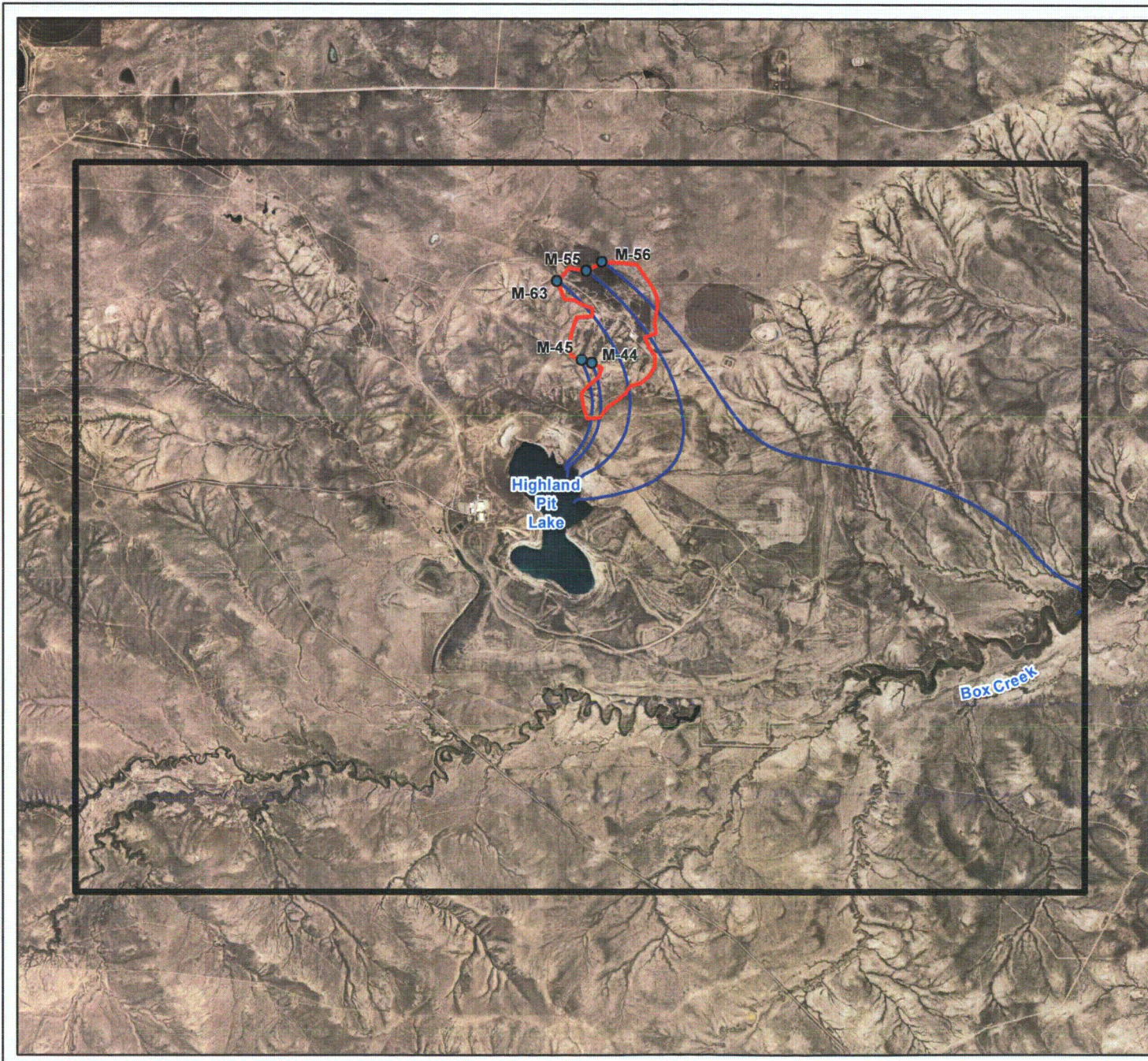
**Figure 6**  
**Hydraulic Head**  
**in the 20-Sand**  
**Cameco Resources**



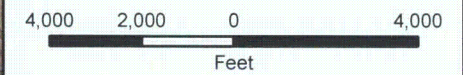




**Figure 7**  
**Particle Pathlines**  
**in the 30-Sand**  
**Cameco Resources**







### Legend

- Velocity (ft/year)
- Mine Unit-B
- Model Domain

**Figure 8**  
**Groundwater Velocities**  
**in the 30-Sand**  
**Cameco Resources**

